



## Early View

Original article

### **CX3CR1-fractalkine axis drives kinetic changes of monocytes in fibrotic interstitial lung diseases**

Flavia R. Greffo, Valeria Viteri-Alvarez, Marion Frankenberger, Daniela Dietel, Almudena Ortega-Gomez, Joyce S. Lee, Anne Hilgendorff, Jürgen Behr, Oliver Soehnlein, Oliver Eickelberg, Isis E. Fernandez

Please cite this article as: Greffo FR, Viteri-Alvarez V, Frankenberger M, *et al.* CX3CR1-fractalkine axis drives kinetic changes of monocytes in fibrotic interstitial lung diseases. *Eur Respir J* 2019; in press (<https://doi.org/10.1183/13993003.00460-2019>).

This manuscript has recently been accepted for publication in the *European Respiratory Journal*. It is published here in its accepted form prior to copyediting and typesetting by our production team. After these production processes are complete and the authors have approved the resulting proofs, the article will move to the latest issue of the ERJ online.

# **CX3CR1-fractalkine axis drives kinetic changes of monocytes in fibrotic interstitial lung diseases**

Flavia R. Greiffo<sup>1</sup>, Valeria Viteri-Alvarez<sup>1</sup>, Marion Frankenberger<sup>1</sup>, Daniela Dietel<sup>1</sup>,  
Almudena Ortega-Gomez<sup>2</sup>, Joyce S. Lee<sup>3</sup>, Anne Hilgendorff<sup>1,4,5,10</sup>, Jürgen Behr<sup>6,7</sup>,  
Oliver Soehnlein<sup>2,8,9</sup>, Oliver Eickelberg<sup>1,3#\*</sup> and Isis E. Fernandez<sup>1,10#\*</sup>

<sup>1</sup>Comprehensive Pneumology Center, Ludwig-Maximilians University (LMU), University Hospital Grosshadern, and Helmholtz Zentrum München; Member of the German Center for Lung Research (DZL), Munich, Germany

<sup>2</sup>Institute for Cardiovascular Prevention, Ludwig-Maximilians University (LMU), Munich, Germany

<sup>3</sup>Division of Pulmonary Sciences and Critical Care Medicine, Department of Medicine, University of Colorado - Anschutz Medical Campus

<sup>4</sup>Department of Neonatology, Perinatal Center Grosshadern Ludwig-Maximilians University, Munich, Germany

<sup>5</sup>Center for Comprehensive Developmental Care, Dr. von Haunersches Children's Hospital University, Hospital Ludwig-Maximilians University, Munich, Germany

<sup>6</sup>Asklepios Fachkliniken München-Gauting, Munich, Germany

<sup>7</sup>Comprehensive Pneumology Center, Medizinische Klinik und Poliklinik V, Klinikum der Ludwig-Maximilians Universität (LMU), Member of the German Center of Lung Research (DZL), Munich, Germany

<sup>8</sup>Deutsches Zentrum für Herz-Kreislaufforschung (DZHK), partner site Munich Heart Alliance

<sup>9</sup>Department of Physiology and Pharmacology, Karolinska Institute, Stockholm, Sweden

<sup>10</sup>CPC-M bioArchive, Helmholtz Zentrum München, Comprehensive Pneumology Center (CPC), Helmholtz Zentrum München, 81377 Munich, Germany, Member of the German Center for Lung Research (DZL)

#These authors contributed equally.

\*To whom correspondence should be addressed: Isis E. Fernandez, Comprehensive Pneumology Center, Ludwig-Maximilian University and Helmholtz Zentrum München, Max-Lebsche-Platz 31, 81377 München, Germany, Tel.: 0049(89)31871663; Fax: 0049(89)31874661; Email: [isis.fernandez@helmholtz-muenchen.de](mailto:isis.fernandez@helmholtz-muenchen.de), or Oliver Eickelberg, University of Colorado Anschutz Medical Campus, Aurora, Colorado, Anschutz Medical Campus, 12700 E. 19<sup>th</sup> Avenue, RC 2, Room 9C03, Box C272, 800045 Aurora, CO, USA, Tel.: 001(303)7244075; Fax: 001(303)7246042; Email: [oliver.eickelberg@ucdenver.edu](mailto:oliver.eickelberg@ucdenver.edu)

### **Take-Home Message**

The compartmental imbalance of fractalkine mediates the migration of non-classical monocytes into fibrotic lung tissues. Furthermore, non-classical monocytes-derived cells show a M2-like and phagocytic phenotype in ILD lungs.

**Running title:** CX3CR1-fractalkine axis in interstitial lung diseases

**Sources of support:** This work was supported by the Helmholtz Association, German Center for Lung Research (DZL), the CPC Research School, and an ERS Short term fellowship (to FRG).

**Key-words:** lung fibrosis, immune cells, receptor-ligand interaction, monocyte-derived cells, macrophages.

## **ABSTRACT**

Circulating immune cell populations have been shown to contribute to interstitial lung disease (ILD). In this study, we analyzed circulating and lung resident monocyte populations, and assessed their phenotype and recruitment from the blood to the lung in ILD. Flow cytometry analysis of blood samples for quantifying circulating monocytes was performed in 105 subjects: 83 with ILD (n = 36, 28, and 19 for non-specific interstitial pneumonia, hypersensitivities pneumonitis, and connective-tissue disease-associated ILD, respectively), as well as 22 controls. Monocyte localization and abundance were assessed by immunofluorescence and flow cytometry of lung tissue. Monocyte populations were cultured either alone or with endothelial cells to assess fractalkine-dependent transmigration pattern. We show that circulating classical monocytes (CM) were increased in ILD compared with controls, while non-classical monocytes (NCM) were decreased. CM abundance inversely correlated, while NCM abundance positively correlated, with lung function. Both CCL2 and CX3CL1 concentrations were increased in plasma and blood of ILD patients. Fractalkine co-localized with ciliated bronchial epithelial cells, thereby creating a chemoattractant gradient towards the lung. Fractalkine enhanced endothelial transmigration of NCM in ILD samples only. Immunofluorescence, as well as flow cytometry, showed an increased presence of NCM in fibrotic niches in ILD lungs. Moreover, NCM in the ILD lungs expressed increased CX3CR1, M2-like, and phagocytic markers. Taken together, our data support that in ILD, fractalkine drives the migration of CX3CR1<sup>+</sup> NCM to the lungs, thereby perpetuating the local fibrotic process.

## **INTRODUCTION**

Interstitial lung disease (ILD) comprises over 200 parenchymal disorders, characterized by diffuse interstitial abnormalities and inflammation. ILD can occur in idiopathic forms or as a result of known triggers, such as environmental exposures to inhaled toxins, genetic, autoimmune, or infectious triggers. Some ILD subtypes, such as nonspecific interstitial pneumonia (NSIP), hypersensitivity pneumonitis (HP), or connective tissue disease-associated ILD (CTD-ILD) may develop into a progressive-fibrotic phenotype with extracellular matrix accumulation that causes impaired gas exchange and leads to respiratory failure [1]. To date, treatment regimen for ILD consists of drugs that suppress an overactive immune system. While recent studies have suggested that nintedanib leads to better preservation of lung function in ILD [2], the therapeutic response relies on the type of diagnosis and disease severity. Irrespective of the underlying cause for ILD, changes in monocyte or macrophage populations can lead to uncontrolled production of cytokines and growth factors that contribute to lung fibrosis [3, 4]. In IPF, absolute and relative numbers of circulating monocytes strongly associate with decreased survival [5].

Human monocytes can be divided into classical (CM), intermediate (IM), and non-classical monocytes (NCM) [6]. CM are defined as  $CD14^{+++}CD16^{+}$  and  $CCR2^{hi}CX3CR1^{low}$  [7]. CM are well investigated, as they account for ~85% of the total monocyte population in humans [7, 8]. Chemokine receptor type 2 (CCR2) mediates mobilization of CM out of the bone marrow to the peripheral blood [7, 8]. NCM phenotype is defined as  $CD14^{+}CD16^{++}$  and  $CCR2^{low}CX3CR1^{hi}$  [7]. In particular, NCM express high levels of CX3C chemokine receptor type 1 (CX3CR1), which has a unique and exclusive ligand: fractalkine (CX3CL1) [9]. CX3CR1 is needed to actively and continuously patrol the luminal side of the vasculature and to remove damaged cells and debris [10].

A recent scRNA-seq study reported that a transitional monocyte-derived cell that expresses CX3CR1 gives rise to a disease-associated macrophage in lung fibrosis. This CX3CR1<sup>+</sup> CD68<sup>+</sup> macrophage transitions into an alveolar identity, localizes to the fibrotic niche, where it exerts a pro-fibrotic effect by driving fibroblast accumulation and enhancing fibrosis [11]. In liver fibrosis, CX3CR1<sup>+</sup> non-classical monocytes replenish tissue macrophage pools and regulate immune responses to injury and infection via M2 differentiation [12, 13]. In kidney fibrosis, CX3CR1<sup>+</sup> non-classical monocytes cells induce the generation of reactive oxygen species (ROS) and the production of fibrotic mediators, such as transforming growth factor beta-1 (TGF- $\beta$ 1) or collagen-I [14, 15]. The abundances, specific phenotypes or lung recruitment patterns of monocytes are largely unclear. Here, we sought to characterize monocyte abundances and phenotypes in blood and lung tissue of ILD patients of different origins, explore and characterize the functions of the CX3CR1-fractalkine axis in circulating non-classical monocytes, and their contributions to tissue-resident phagocyte populations in human ILD samples.

## **METHODS**

For a detailed description, please refer to the online supplement. All reagents used here are listed in supplemental table S1.

### **Subjects**

The study was performed in accordance with protocols approved by the Ludwig-Maximilians Universität München Ethic's Review Board (Ethikkommission numbers 180-14 and 454-12). All subjects provided informed written consent for the research study and molecular testing. A total of 105 patients were included in this study (Table 1).

### **Flow Cytometry**

Peripheral blood mononuclear cells (PBMCs) were isolated by density gradient (Lymphoprep<sup>TM</sup>). Tissue homogenate CD45<sup>+</sup> cells were selected by MicroBeads (Miltenyi Biotec; Bergisch Gladbach, Germany). Peripheral and tissue monocytes subsets were detected by flow cytometry.

### **Methylprednisolone assay**

To investigate the glucocorticoid effect on monocytes subsets, and understand if glucocorticoids affect mature monocyte phenotype, we performed experiments with isolated monocytes from controls and treated them with different doses of methylprednisolone, at 3 and 24 hours.

### **Protein quantification**

CC Chemokine Ligand 2 (CCL2) and fractalkine (CX3CL1) (Quantikine Kit R&D Systems, Abingdon, UK) were used to quantify chemokines levels in plasma and tissue homogenate by enzyme-linked immunosorbent assay (ELISA).

## **Immunofluorescence**

Tissue tumor-free areas (control), NSIP, HP and CTD-ILD explanted lungs were used to localize and quantify tissue myeloid cells.

## **Monocyte adhesion assay**

Immortalized murine endothelial cells were used to analyze monocyte adhesion. Monocytes were isolated from PBMCs using the Pan Monocyte Isolation Kit followed by CD16 MicroBeads (Miltenyi Biotec; Bergisch Gladbach, Germany), resulting in a separation of CD14<sup>+</sup> and CD16<sup>+</sup> monocytes. We performed a competitive assay between CD16<sup>+</sup> monocytes from ILD subjects and CD16<sup>+</sup> monocytes from control (supplemental figure S1).

## **Monocyte migration assay**

Isolated monocytes were seeded into a transwell to verify whether migration of monocyte subsets respond to different stimuli. Four different conditions were added in the lower chamber. Migration index was calculated after 3 hours (supplemental figure S1).

## **Statistical analysis**

Results are presented as box and whiskers vertical graphs with mean  $\pm$  standard deviation. For normality distribution, Shapiro–Wilk test was performed. Therefore, three group comparisons were analyzed using the Kruskal-Wallis' test followed by Dunn's multiple comparison test. Two group comparisons were analyzed using the Mann-Whitney test. Associations between variables were established using linear regression and Pearson correlation. GraphPad Prism (version 7.0, GraphPad Software; San Diego, CA, USA) was used for statistical analyzes, and significance was defined as p less than 0.05.

## RESULTS

A table of patient characteristics and including additional values and statistical differences between groups can be found in the online supplemental data (Table S1 and 2).

### Dynamic changes of circulating monocytes in ILD

Monocytes were measured and quantified in circulating PBMCs (Figure 1A). Classical monocytes, defined as HLA-DR<sup>+</sup>CD14<sup>+++</sup>CD16<sup>-</sup>, were significantly increased in NSIP and HP patients compared with controls (Figure 1B). In contrast, the abundance of intermediate monocytes, defined as HLA-DR<sup>+</sup>CD14<sup>+</sup>CD16<sup>+</sup>, were not different comparing NSIP, HP, CTD-ILD, and controls (Figure 1C). Non-classical monocytes, defined as HLA-DR<sup>+</sup>CD14<sup>+</sup>CD16<sup>++</sup>, were significantly decreased in NSIP, HP, and CTD-ILD subjects, compared with controls (Figure 1D). We next correlated the percentages of circulating monocytes with diffusing lung capacity for carbon monoxide (DL<sub>CO</sub>) and forced vital capacity (FVC). The abundance of CM and NCM were significantly correlated, negatively and positively with DL<sub>CO</sub> (% of predicted), respectively (Figure 1E-G). The abundance of CM, IM, or NCM was not significantly correlated with forced vital capacity (FVC) (% of predicted) (supplemental figure S2). To understand whether monocyte subset abundances were associated with treatment, we grouped combined all NSIP, HP, and CTD-ILD as ILD, and analyzed treatment effects as follows: 1) Naïve (not treated), 2) Immunosuppressive treatment including azathioprine, methotrexate, mycophenolic acid, and rituximab (Imm), 3) Glucocorticoid treatment (GC), and 4) Combined immunosuppressive and glucocorticoid treatment (Imm+GC). This analysis revealed that CM were highest in ILD patients treated with GC and Imm+GC, compared with controls, as well in patients with GC-treated patients compared with treatment-naïve (Figure 2A). IM abundance was not different between any groups (Figure 2B). NCM were lowest in

ILD patients treated with GC and Imm+GC, compared with controls (Figure 2C), as well in GC-treated patients when compared with treatment-naïve (Figure 2C).

Since peripheral monocyte abundance was associated specifically with GC therapy, we next examined whether glucocorticoids influenced monocyte subsets using the following two approaches. First, we treated whole blood with methylprednisolone (at concentrations of  $10^{-12}$ M,  $10^{-9}$ M, and  $10^{-6}$ M) and analyzed monocyte phenotypes by flow cytometry. After 3 hours of treatment, abundance or phenotype of CM, IM, or NCM were not altered compared with untreated blood (Figure 2E). When we isolated PBMCs and treated those for 24 hrs with methylprednisolone (at concentrations of  $10^{-12}$ M,  $10^{-9}$ M, and  $10^{-6}$ M), we observed an increased number of intermediate monocytes treated with  $10^{-9}$  and  $10^{-6}$ M of methylprednisolone compared with untreated PBMC (Figure 2E).

### **Expression of canonical kinetic and scavenger receptors in non-classical monocytes in ILD**

To fully characterize the immunophenotype of these monocyte populations in ILD, we explored the expression of receptor profiles known to distinguish monocyte subsets (CCR2 in classical monocytes, CX3CR1 in non-classical monocytes, and CD163 scavenger receptor in myeloid lineages) (Figure 3). We observed that CCR2 mean fluorescence intensity (MFI) in CM was significantly decreased in ILD subjects compared with controls (Figures 3B-E and supplemental figure S2). CX3CR1 was decreased in ILD subjects in CM and NCM compared with controls (Figures 3C and 3F, supplemental figure S2). In contrast, the scavenger receptor CD163 expression was increased in NCM in ILD subjects compared with controls (Figures 3D and 3G, and supplemental figure S2).

### **CX3CL1 increased non-classical monocyte migration and accumulation in the lung parenchyma of ILD patients**

Mobilization of monocyte populations into and out of the circulation into target organs occurs in a chemokine-controlled fashion [7, 16]. In order to understand the altered abundance of classical and non-classical monocytes in the circulation of ILD patients, we investigated chemotactic gradients that might influence peripheral abundance, in particular CCL2 and fractalkine (CX3CL1) in plasma and lung homogenates of controls and ILD. Both CCL2 and CX3CL1 concentrations were significantly increased in plasma of ILD patients compared with controls (Figure 4A, B). Only CX3CL1 concentrations, however, were significantly higher in lung tissues of ILD patients compared with controls (Figure 4B). In control and ILD, CX3CL1 levels were higher in the lung tissue than in the plasma.

We next evaluated the effects of this chemoattractant gradient of fractalkine (CX3CL1), and receptor responsiveness to the ligand, in co-cultures of primary monocytes from control and ILD patients with activated endothelial cells. We observed that CX3CL1 did not influence NCM adhesion, but migration (figure 4C). In ILD subjects only, NCM migration was significantly increased in the presence of fractalkine (figure 4D). Blockage of fractalkine (CX3CL1) with a monoclonal antibody reversed this effect (Figure 4D). CCL2 had no influence on NCM adhesion or migration (supplemental figure 1).

To characterize localization of monocytes in the lung, we next performed immunofluorescence staining of lung tissue from ILD subjects and controls. ILD sections identified CD14<sup>+</sup>CD16<sup>+</sup> double positive cells in lung parenchyma outside vessels (Figure 5A). The number of CD14<sup>+</sup>CD16<sup>+</sup> myeloid cells was significantly increased in the lung parenchyma of explanted ILD subjects compared with controls (Figure 5A). Immunofluorescence staining showed that CD14<sup>+</sup>CD16<sup>+</sup> double positive cells expressed CX3CR1 and CD163 in ILD (Figure 5B-C), as well as the abundant

presence of CX3CR1<sup>+</sup>CD163<sup>+</sup> in ILD lung tissue (Figure 5D and S3 in the data supplement). CX3CR1<sup>+</sup> cells co-expressed the M2 marker CD68 (figure 5E).

### **Increased abundance of pro-fibrotic CD14<sup>+</sup>CD16<sup>++</sup> myeloid cells in the ILD lung**

To unequivocally quantify the abundance of CD14<sup>+</sup>CD16<sup>++</sup> double positive cells in the lung and characterize their phenotype and function, we performed flow cytometry of single cell suspensions of lung tissue. We observed a significant increase in the percentages and absolute cell numbers (cell/ $\mu$ l) of CD14<sup>+</sup>CD16<sup>++</sup> double positive cells in ILD lungs compared with controls (Figure 6A). To explore the phenotypic and functional features of tissue NCM, we analyzed the expression of mature myeloid markers (CD206) and receptors involved in apoptotic cell clearance and phagocytosis (AXL, MERTK). Flow cytometry analysis showed that tissue NCM in ILD and control expressed CX3CR1 (Figure 6B). Tissue NCM from ILD lungs expressed higher levels of MERTK and CD206 than CD14<sup>+</sup> cells compared with controls (Figure 6B). Immunofluorescence analysis revealed the expression of AXL in CD14<sup>+</sup>CD16<sup>+</sup> cells in ILD (Figure 6C). Finally, we performed immunofluorescence staining in ILD lungs to determine which lung cell type contributes to increased fractalkine (CX3CL1) levels. We observed that CX3CL1 was highly expressed in acetylated tubulin-positive airway epithelial cells, but not in collagen-1-positive mesenchymal cells or von Willebrand factor-positive endothelial cells (Figure 6D).

## **DISCUSSION**

Here, we demonstrate the functional implications of the CX3CR1-fractalkine axis on the abundance and recruitment of monocyte populations in human ILD (Figure 7). We demonstrate higher and lower numbers of circulating classical (CM) and non-classical monocytes (NCM), respectively, in ILD of multiple different origin. In addition, CM and NCM numbers in peripheral blood correlate with lung function

(DL<sub>CO</sub>) in a negative and positive manner, respectively. These altered abundances of circulating monocytes are the result of predominantly corticosteroid treatment, suggesting shifting monocyte populations induced by treatment. Functional studies indicate that NCM migration is mediated by fractalkine (CX3CL1), and that ciliated bronchial epithelial cells constitute the local source of fractalkine secretion, creating a chemoattractant gradient of CX3CL1 towards the fibrotic lung. The CD14<sup>+</sup>CD16<sup>++</sup> NCM are abundant in fibrotic ILD lungs and express CX3CR1 and M2-like markers. The percentages of monocyte subsets are highly conserved in healthy humans [7]. In acute or chronic diseases, however, percentages of monocyte subsets may vary and respond differently as a consequence of pathological stimuli [17]. Our results show that CM were significantly increased, whereas NCM were significantly decreased, in the peripheral blood in ILD compared with controls. We observed that patients with higher numbers of CM had worse lung function (as measured by DL<sub>CO</sub>), while higher numbers of NCM indicated better lung function. Importantly, a recent abstract report of patients from the MESA (Multi-Ethnic Study of Atherosclerosis) study showed that increased abundance of monocytes in the peripheral blood in subclinical ILD is associated with early interstitial lung abnormalities and lower FVC [18], supporting the role of altered monocyte counts even in early stages of disease. This study, however, did not report on specific monocyte subtypes. Thus, those data may be driven by the increased abundance of CM in ILD patients, which might occur even at early stages in treatment-naïve patients. More recently, circulating CD14<sup>+</sup> classical monocytes have been suggested to be a potent cellular biomarker in idiopathic pulmonary fibrosis (IPF) [5]. Monocytes were quantified in the peripheral blood of IPF patients from six different cohorts showing that high abundance of CD14<sup>+</sup> classical monocytes correlated with poor disease outcome [5]. To this end, our cohort is composed of severe and end-stage ILD patients. Concomitant with those previous

studies, our data shows an increased abundance of classical monocytes in NSIP and HP patients compared with control, as well as a negative correlation with DL<sub>CO</sub>. Of note, while monocyte counts correlated with DL<sub>CO</sub>, they did not correlate with FVC, which may be explained by pulmonary vascular changes, differences in clinical handling of IPF and non-IPF ILD, their specific immune subsets, or highly dynamic changes of pro-fibrotic monocytes influenced by treatment.

We were interested to understand whether immunomodulatory therapies affected monocyte counts and thus stratified ILD patients according to treatment regimen. Glucocorticoid therapy has been reported to affect monocyte populations in the peripheral blood [19, 20], and we observed significant effects of GC treatment on CM and NCM populations. To further interrogate these effects, we treated whole blood as well as isolated PBMCs, with methylprednisolone *in vitro*. Interestingly, we observed that GC treatment only affected IM, but not CM or NCM abundances, suggesting that the *in vivo* effects are not due to shifting maturation/differentiation of circulating monocytes, but rather to changes in transmigration patterns into/out of e.g. the lung. In line with our experiments, previous studies have described that the abundance of IM is associated with systemic glucocorticoid treatment in uveitis patients [21]. Specifically, the following scenarios may explain the changes of circulating CM and NCM cells in ILD [22]: GC-mediated emigration of CD14<sup>++</sup>CD16<sup>-</sup> from the bone marrow [23], a transitory stage of differentiation from CD14<sup>++</sup>CD16<sup>-</sup> to CD14<sup>+</sup>CD16<sup>++</sup> [24], a lack of peripheral maturation of CD14<sup>++</sup>CD16<sup>-</sup> cells into CD14<sup>+</sup>CD16<sup>++</sup> cells [25], or the depletion of CD14<sup>+</sup>CD16<sup>++</sup> monocytes in circulation as they move into tissues [25].

Our phenotypic characterization of monocytes in the peripheral blood showed that MFI levels of CCR2 and CX3CR1 were decreased in CM, whereas only CX3CR1 was decreased in NCM in ILD patients. When chemokine receptors are engaged in

chemotaxis, they can be transiently removed from the cell surface by ligand-receptor internalization or clathrin-mediated endocytosis [26], which might explain the decrease of CCR2 and CX3CR1 in our data. In contrast, we detected an increased expression of CD163 in NCM in ILD. CD163 is a scavenger receptor, and marker of M2 activation [27], expressed by CD14<sup>+</sup> circulating cells in scleroderma-ILD patients, and in the tissue of several types of ILD [28, 29].

We observed significantly increased plasma levels of CCL2 and fractalkine (CX3CL1) in ILD. When comparing the circulatory and lung compartments, CCL2 was more abundant in the plasma, suggesting active monocyte recruitment from the bone marrow. This supports the increased numbers of CM in the circulation, and decreased levels of CCR2 by receptor internalization, as previously described [30]. In contrast, fractalkine levels were higher in lungs than plasma in ILD. Functional experiments demonstrated increased migration of NCM in the presence of fractalkine in ILD samples only. This effect was reversed when a monoclonal antibody against CX3CL1 was added. Monocyte recruitment responds to receptor-ligand interaction [31], our data thus support that NCM migration driven by CX3CL1 is specifically increased during injury. Increasing evidence supports the contributing role of the airway epithelium in diffuse parenchymal lung disease [32-34]. Here we showed that the main source of CX3CL1 in ILD lungs are acetylated-tubulin positive (i.e. ciliated) bronchial epithelial cells. These findings are consistent with a recent study demonstrating that CX3CL1 is expressed by lung epithelial cells in scleroderma-ILD [35] and supports bronchial epithelium-immune crosstalk as an important regulator of tissue injury and fibrosis [36, 37].

In the current study, we also performed FACS analysis of single cell suspensions of lung tissue, and detected increased numbers of tissue NCM in ILD patients. While we are limited in unequivocally determining whether this population constitutes

particularly sticky intravascular circulating or true tissue-invading monocytes, similar populations have been recently reported using single cell RNAseq data. Providing the first extensive single cell landscape of human fibrotic lungs, Reyfman et al. [37] and Habermann et al. [38] reported a distinct, novel population of pro-fibrotic alveolar macrophages exclusively present in patients with fibrosis. These studies has been extended by the largest scRNA-seq study available to-date using diseased lungs and profiling more than 300.000 cells from 32 IPF lungs, 18 COPD lungs, and 29 controls [39]. In this study, the authors detected the presence of pro-fibrotic monocyte-derived macrophages and NCM in fibrotic lungs, although no intra- or extravascular distinction was made. Finally, Travaglini et al. [40] recently provided a human lung cell atlas during fibrosis. By profiling simultaneously blood and tissue, they identified lung-specific immune gene expression profiles and their changes during homing, local signaling interactions, including sources and targets of chemokines in immune cell trafficking. Importantly, they detected the presence of tissue-invading extravascular NCM and their CX3CR1-mediated homing in response to CX3CL1-expressing endothelial cells and airway epithelial cells, confirming our findings [40].

Along these lines, scRNA-seq studies in mice have reported a transitional CX3CR1<sup>+</sup> monocyte-derived cell giving rise to fibrotic-associated macrophages in the lung [41]. This CX3CR1<sup>+</sup> CD68<sup>+</sup> macrophage transitions into an alveolar identity, and localizes in the fibrotic niche exerting a local pro-fibrotic effect by driving fibroblast accumulation, myofibroblast differentiation, and enhancing fibrosis [11]. Another complimentary genetic lineage tracing study showed that increases in alveolar macrophages during fibrosis are attributable to recruited monocytes-derived cells carrying a fibrotic transcriptome profile [42]. Along this line, our cell culture models using primary lung fibroblasts isolated from fibrotic lungs show increased mRNA expression of pro-fibrotic markers in the presence of CX3CR1<sup>+</sup> monocytes and

CX3CL1, when compared with CX3CR1<sup>+</sup> monocytes alone (*data not shown*). Furthermore, CX3CR1 knockout mice are protected from fibrosis by decreasing mRNA and protein levels of TGF- $\beta$  [43].

The CX3CL1/Fractalkine is identified as “find-me signal”, from injured pre-apoptotic cells [44]. Therefore, to investigate the functional implication of this finding, we assessed the expression of TAM (TYRO3, AXL and MERTK) family receptors [45] in myeloid cells in the lung. Linked to CD163 scavenger receptor, AXL and MERTK signaling contributes to the “eat-me signals”, which recognize injured and apoptotic cells for phagocytosis by receptor activation [46]. We found that only in ILD, CD14<sup>+</sup>CD16<sup>+</sup> cells expressed AXL. Our results are consistent with previous findings showing that immune cells localized in the fibrotic lung parenchyma are AXL positive [47]. Furthermore, we show that CD14<sup>+</sup>CD16<sup>++</sup> myeloid cells in the ILD lung expressed CD163, MERTK, macrophage mannose receptor CD206, CD68 and CX3CR1, as supported by others [48].

In conclusion, this study identified a chemotactic gradient of fractalkine that mediates the migration of CX3CR1<sup>+</sup> NCM into human fibrotic lungs. Furthermore, NCM-derived cells expressed phagocytosis markers and an M2-like phenotype in the ILD lungs. Targeting CX3CR1-fractalkine axis may aid the management of end-stage ILD and provide novel therapeutic strategies to either restore monocyte function or modulate recruitment.

## **ACKNOWLEDGEMENTS**

We gratefully acknowledge the provision of human biomaterial and clinical data from the CPC-M bioArchive and its partners at the Asklepios Biobank Gauting, the Klinikum der Universität München, the Helmholtz Zentrum München and the Ludwig-Maximilians-Universität München. We thank Dr. Davide Biondini for fruitful clinical discussions (Department of Cardiac Thoracic and Vascular Sciences, University of Padua, Padua, Italy). We thank the CPC Research School (grant writing challenge), the Helmholtz Association, and German Center for Lung Research (DZL) for supporting and funding this work. We acknowledge the support of the European Respiratory Society - ERS Short-Term Research Fellowship (to FRG).

## **AUTHOR CONTRIBUTIONS**

Conception and design: FRG, OE and IEF

Experimental work, analysis, and interpretation: FRG, MF, DD, VVA, JB, OS, OE, and IEF

Intellectual content: FRG, MF, DD, AOG, JSL, AH, JB, OS, OE and IEF

Drafting the manuscript: FRG, OE and IEF

Editing the manuscript: FRG, OE and IEF

## REFERENCES

1. Travis, W.D., et al., *An official American Thoracic Society/European Respiratory Society statement: Update of the international multidisciplinary classification of the idiopathic interstitial pneumonias*. Am J Respir Crit Care Med, 2013. **188**(6): p. 733-48.
2. Flaherty, K.R., et al., *Nintedanib in Progressive Fibrosing Interstitial Lung Diseases*. N Engl J Med, 2019.
3. Wynn, T.A. and K.M. Vannella, *Macrophages in Tissue Repair, Regeneration, and Fibrosis*. Immunity, 2016. **44**(3): p. 450-462.
4. Zhou, X. and B.B. Moore, *Location or origin? What is critical for macrophage propagation of lung fibrosis?* Eur Respir J, 2018. **51**(3).
5. Scott, M.K.D., et al., *Increased monocyte count as a cellular biomarker for poor outcomes in fibrotic diseases: a retrospective, multicentre cohort study*. Lancet Respir Med, 2019. **7**(6): p. 497-508.
6. Passlick, B., D. Flieger, and H.W. Ziegler-Heitbrock, *Identification and characterization of a novel monocyte subpopulation in human peripheral blood*. Blood, 1989. **74**(7): p. 2527-34.
7. Shi, C. and E.G. Pamer, *Monocyte recruitment during infection and inflammation*. Nat Rev Immunol, 2011. **11**(11): p. 762-74.
8. Patel, A.A., et al., *The fate and lifespan of human monocyte subsets in steady state and systemic inflammation*. J Exp Med, 2017. **214**(7): p. 1913-1923.
9. Geissmann, F., et al., *Development of monocytes, macrophages, and dendritic cells*. Science, 2010. **327**(5966): p. 656-61.
10. Auffray, C., et al., *Monitoring of blood vessels and tissues by a population of monocytes with patrolling behavior*. Science, 2007. **317**(5838): p. 666-70.
11. Aran, D., et al., *Reference-based analysis of lung single-cell sequencing reveals a transitional profibrotic macrophage*. Nat Immunol, 2019. **20**(2): p. 163-172.
12. Aspinall, A.I., et al., *CX(3)CR1 and vascular adhesion protein-1-dependent recruitment of CD16(+) monocytes across human liver sinusoidal endothelium*. Hepatology, 2010. **51**(6): p. 2030-9.
13. Brempelis, K.J. and I.N. Crispe, *Infiltrating monocytes in liver injury and repair*. Clin Transl Immunology, 2016. **5**(11): p. e113.
14. Hochheiser, K., et al., *Exclusive CX3CR1 dependence of kidney DCs impacts glomerulonephritis progression*. J Clin Invest, 2013. **123**(10): p. 4242-54.
15. Shimizu, K., et al., *Fractalkine and its receptor, CX3CR1, promote hypertensive interstitial fibrosis in the kidney*. Hypertens Res, 2011. **34**(6): p. 747-52.
16. Imhof, B.A. and M. Aurrand-Lions, *Adhesion mechanisms regulating the migration of monocytes*. Nat Rev Immunol, 2004. **4**(6): p. 432-44.
17. Boyette, L.B., et al., *Phenotype, function, and differentiation potential of human monocyte subsets*. PLoS One, 2017. **12**(4): p. e0176460.
18. Anna Podolanczuk, E.B., John Kim, Eric Hoffman, Ganesh Raghu, Steven Kawut, Margaret Doyle, Russell Tracy, Graham Barr, Nancy Jenny, David Lederer, *Innate and adaptive immunity in subclinical ILD in the Multi-Ethnic Study of Atherosclerosis*, in *International Colloquium on Lung and Airway Fibrosis (ICLAF)*. 2018: Pacific Grove, CA.
19. Ehrchen, J., et al., *Glucocorticoids induce differentiation of a specifically activated, anti-inflammatory subtype of human monocytes*. Blood, 2007. **109**(3): p. 1265-74.

20. Varga, G., et al., *Glucocorticoids induce an activated, anti-inflammatory monocyte subset in mice that resembles myeloid-derived suppressor cells*. J Leukoc Biol, 2008. **84**(3): p. 644-50.
21. Liu, B., et al., *CD14<sup>++</sup>CD16<sup>+</sup> Monocytes Are Enriched by Glucocorticoid Treatment and Are Functionally Attenuated in Driving Effector T Cell Responses*. J Immunol, 2015. **194**(11): p. 5150-60.
22. Zhong, H., et al., *CD16<sup>+</sup> monocytes control T-cell subset development in immune thrombocytopenia*. Blood, 2012. **120**(16): p. 3326-35.
23. Rhen, T. and J.A. Cidlowski, *Antiinflammatory action of glucocorticoids--new mechanisms for old drugs*. N Engl J Med, 2005. **353**(16): p. 1711-23.
24. Ziegler-Heitbrock, H.W., *Heterogeneity of human blood monocytes: the CD14<sup>+</sup> CD16<sup>+</sup> subpopulation*. Immunol Today, 1996. **17**(9): p. 424-8.
25. Martinez, F.O., *The transcriptome of human monocyte subsets begins to emerge*. J Biol, 2009. **8**(11): p. 99.
26. Springer, T.A., *Traffic signals for lymphocyte recirculation and leukocyte emigration: the multistep paradigm*. Cell, 1994. **76**(2): p. 301-14.
27. Pilling, D., et al., *Identification of markers that distinguish monocyte-derived fibrocytes from monocytes, macrophages, and fibroblasts*. PLoS One, 2009. **4**(10): p. e7475.
28. Mathai, S.K., et al., *Circulating monocytes from systemic sclerosis patients with interstitial lung disease show an enhanced profibrotic phenotype*. Lab Invest, 2010. **90**(6): p. 812-23.
29. Prasse, A., et al., *A vicious circle of alveolar macrophages and fibroblasts perpetuates pulmonary fibrosis via CCL18*. Am J Respir Crit Care Med, 2006. **173**(7): p. 781-92.
30. Cardona, A.E., et al., *Scavenging roles of chemokine receptors: chemokine receptor deficiency is associated with increased levels of ligand in circulation and tissues*. Blood, 2008. **112**(2): p. 256-63.
31. Haribabu, B., et al., *Function and regulation of chemoattractant receptors*. Immunol Res, 2000. **22**(2-3): p. 271-9.
32. Seibold, M.A., et al., *A common MUC5B promoter polymorphism and pulmonary fibrosis*. N Engl J Med, 2011. **364**(16): p. 1503-12.
33. Mathai, S.K., et al., *Desmoplakin Variants Are Associated with Idiopathic Pulmonary Fibrosis*. Am J Respir Crit Care Med, 2016. **193**(10): p. 1151-60.
34. Habel, D.M., et al., *CCR10<sup>+</sup> epithelial cells from idiopathic pulmonary fibrosis lungs drive remodeling*. JCI Insight, 2018. **3**(16).
35. Hoffmann-Vold, A.M., et al., *Augmented concentrations of CX3CL1 are associated with interstitial lung disease in systemic sclerosis*. PLoS One, 2018. **13**(11): p. e0206545.
36. Lechner, A.J., et al., *Recruited Monocytes and Type 2 Immunity Promote Lung Regeneration following Pneumonectomy*. Cell Stem Cell, 2017. **21**(1): p. 120-134 e7.
37. Reyfman, P.A., et al., *Single-Cell Transcriptomic Analysis of Human Lung Provides Insights into the Pathobiology of Pulmonary Fibrosis*. Am J Respir Crit Care Med, 2018.
38. Habermann A.C., et al., *Single-cell RNA-sequencing reveals profibrotic roles of distinct epithelial and mesenchymal lineages in pulmonary fibrosis*. bioRxiv doi: 10.1101/753806, 2019.
39. Adams T.S., et al., *Single Cell RNA-seq reveals ectopic and aberrant lung resident cell populations in Idiopathic Pulmonary Fibrosis*. bioRxiv doi: 10.1101/759902, 2019.

40. Travaglini K.J., et al., *A molecular cell atlas of the human lung from single cell RNA sequencing*. bioRxiv doi: 10.1101/742320, 2019.
41. Schyns, J., et al., *Non-classical tissue monocytes and two functionally distinct populations of interstitial macrophages populate the mouse lung*. Nat Commun, 2019. **10**(1): p. 3964.
42. Misharin, A.V., et al., *Monocyte-derived alveolar macrophages drive lung fibrosis and persist in the lung over the life span*. J Exp Med, 2017. **214**(8): p. 2387-2404.
43. Ishida, Y., et al., *Essential involvement of the CX3CL1-CX3CR1 axis in bleomycin-induced pulmonary fibrosis via regulation of fibrocyte and M2 macrophage migration*. Sci Rep, 2017. **7**(1): p. 16833.
44. Truman, L.A., et al., *CX3CL1/fractalkine is released from apoptotic lymphocytes to stimulate macrophage chemotaxis*. Blood, 2008. **112**(13): p. 5026-36.
45. Graham, D.K., et al., *The TAM family: phosphatidylserine sensing receptor tyrosine kinases gone awry in cancer*. Nat Rev Cancer, 2014. **14**(12): p. 769-85.
46. Li, W., *Eat-me signals: keys to molecular phagocyte biology and "appetite" control*. J Cell Physiol, 2012. **227**(4): p. 1291-7.
47. Espindola, M.S., et al., *Targeting of TAM Receptors Ameliorates Fibrotic Mechanisms in Idiopathic Pulmonary Fibrosis*. Am J Respir Crit Care Med, 2018.
48. Gibbings, S.L., et al., *Three Unique Interstitial Macrophages in the Murine Lung at Steady State*. American Journal of Respiratory Cell and Molecular Biology, 2017. **57**(1): p. 66-76.

## FIGURE LEGENDS

**Table 1. Clinical demographics.** ILD includes non-specific interstitial pneumonia (NSIP), hypersensitivity pneumonitis (HP), and connective tissue disease-ILD (CTD-ILD). In lung comorbidities: pulmonary artery hypertension (PAH), PAH was determined by echocardiography detecting an increase in mean pulmonary artery pressure >25 mmHg; combined pulmonary fibrosis and emphysema (CPFE). Immunosuppressor treatment includes azathioprine, methotrexate, mycophenolic acid, and rituximab. Data are presented as % and number of affected patients (yes/no). Lung function data are presented as mean±SD, diffusing capacity of the lung for carbon monoxide (DLCO); forced volume capacity of the lung (FVC). \* represents  $p<0.05$  when compared with control \*\* represents  $p<0.01$  when compared with control † represents  $p<0.05$  when compared with NSIP and HP and †† represents  $p<0.01$  when compared with NSIP and HP.

**Figure 1. Dynamic changes of circulating monocytes population in ILD.** a) PBMCs were stained with mAbs, and each monocyte subset was previously defined by HLA-DR<sup>+</sup> cells and gated according to CD14 and CD16 expression, CD14<sup>+++</sup>CD16<sup>-</sup> as classical monocytes, CD14<sup>+</sup>CD16<sup>+</sup> as intermediate monocytes, and CD14<sup>+</sup>CD16<sup>++</sup> as non-classical monocytes. Isotype was used as a negative control and is represented by gray dots; b) Flow cytometry analysis show from total monocytes the percentage of classical monocytes; c) intermediate monocytes; d) non-classical monocytes. Control (n=22), NSIP (n=36), HP (n= 28), CTD-ILD (n=19). Statistical analysis was performed using one-way analysis of variance with non-parametric Kruskal-Wallis test, followed by Dunn's multiple comparison test. \* represents  $p<0.05$ , and \*\* represents  $p<0.01$ , compared with control. e) percentage of classical monocytes correlated with DLCO (% predicted) in ILD (n=58); f)

percentage of intermediate monocytes correlated with DLCO (% predicted) in ILD (n= 58); g) percentage of non-classical monocytes subsets correlated with DLCO (% predicted) in ILD (n= 58). For statistical analysis, p values were calculated by Student's t distribution and Pearson correlation. \* represents  $p<0.05$ , and \*\* represents  $p<0.01$ .

**Figure 2. Circulating mature monocyte abundance is associated with ILD treatment.** PBMCs were stained with mAbs, and each monocyte subset was previously defined by HLA-DR<sup>+</sup> cells and gated according to CD14 and CD16 expression, CD14<sup>+++</sup>CD16<sup>-</sup> as classical monocytes, CD14<sup>+</sup>CD16<sup>+</sup> as intermediate monocytes, and CD14<sup>+</sup>CD16<sup>++</sup> as non-classical monocytes. Flow cytometry analysis show from total monocytes the percentage of a) classical monocytes; b) intermediate monocytes; c) non-classical monocytes. Control (n=22), ILD naïve (n=15), ILD immunosuppressor (Imm) (n=5), ILD glucocorticoid (GC) (n=31), ILD immunosuppressor with glucocorticoid (Imm+GC) (n=32). Statistical analysis was performed using one-way analysis of variance with non-parametric Kruskal-Wallis test, followed by Dunn's multiple comparison test. \* represents  $p<0.05$ , \*\* represents  $p<0.01$  and \*\*\* represents  $p<0.001$ , compared with control or ILD naïve. d) Different concentrations of methylprednisolone were added or not in 100ul of whole blood and incubated for 3h. Flow cytometry was performed to quantify percentages of classical, intermediate and non-classical monocytes. e) Different concentrations of methylprednisolone were added or not in cell culture medium of freshly isolated monocytes. Flow cytometry was performed to quantify percentages of classical, intermediate and non-classical monocytes. For methylprednisolone experiments, n=3. Statistical analysis was performed using non-parametric two-tailed Mann-Whitney t test. \* represents  $p<0.05$  compared with control \*\* represents  $p<0.01$

compared with control \*\*\* represents  $p < 0.001$  compared with 24h without methylprednisolone.

**Figure 3. Circulating monocytes show decreased CX3CR1 and increased CD163 expression in ILD.** Box and whiskers with dot plot diagrams of flow cytometry analysis show the a) mean fluorescence intensity (MFI) of CCR2, CX3CR1 and CD163. b) CCR2<sup>+</sup> classical monocytes; c) CX3CR1<sup>+</sup> classical monocytes; d) CD163<sup>+</sup> classical monocytes; e) CCR2<sup>+</sup> non-classical monocytes; f) CX3CR1<sup>+</sup> non-classical monocytes; g) CD163<sup>+</sup> non-classical monocytes. For A,B, E, F: control (n=20), ILD (n=83). For D and G control (n= 8), ILD (n= 57). Statistical analysis was performed using non-parametric two-tailed Mann-Whitney t test. \*\* represents  $p < 0.01$  and \* represents  $p < 0.05$  compared with control.

**Figure 4. Fractalkine is increased in the lung and drives the migration of non-classical monocytes in ILD.** Enzyme-linked immune assay (ELISA) for CCL2 and fractalkine were performed in lung tissue homogenate. a) CCL2 (pg/mL) in plasma (control n=23, and ILD n=63), and lung tissue (control n=9, and ILD n=28); b) CX3CL1 (ng/mL) in plasma (control n=15, and ILD n=44), and lung tissue (control n=9, and ILD n=29). c) *In vitro* adhesion assay of CD16<sup>+</sup> monocytes on the activated endothelial cells (TNF- $\alpha$ , 4 hours), control wells were used as an indicator of conversion efficiency. Control (n=5) ILD (n=5). d) *In vitro* migration assay of non-classical monocytes, control wells were used as an indicator of conversion efficiency. Control (n=13), ILD (n=14). For functional assays, 3-5 experimental replicates were use in each experiment. Statistical analysis was performed using non-parametric two-tailed Mann-Whitney t test. \* represents  $p < 0.05$  compared with control \*\* represents  $p < 0.01$  compared with control \*\*\* represents  $p < 0.001$  compared with control.

**Figure 5. Non-classical monocytes are increased in the lung parenchyma in ILD.** a) Immunofluorescence triple staining was performed using explanted lungs from control, and ILD. Explanted lungs were stained for CD14 (red), CD16 (green), and Von Willebrand factor (vWF) (white). Squares and arrows show double positive cells; Graphs bars show the quantification of CD14<sup>+</sup> and CD14<sup>+</sup>CD16<sup>+</sup> myeloid cells in the lung parenchyma of control and non-IPF ILD as % of total cells. Control (n= 3), ILD (n=6). b) CX3CR1 (red), CD16 (green), CD14 (white). Squares and arrows show triple positive cells. c) CD163 (red), CD16 (green), CD14 (white). Squares and arrows show triple positive cells. d) CX3CR1 (red), and CD163 (green). e) CX3CR1 (red), and CD68 (green); Red arrows show CX3CR1 positive cells and green arrows show CD68 positive cells. Squares and arrows show double positive cells. Cell nuclei are stained with DAPI (blue). All the pictures were taken using magnification of 20x (scale bar= 50µm), white squares represent higher magnification (scale bar= 10µm). Control (n=3), ILD (n=3). Statistical analysis was performed using non- parametric two-tailed Mann-Whitney t test. \* represents p<0.05 compared with control.

**Figure 6. Fractalkine is expressed by the lung epithelium and non-classical monocytes-derived cells expressed M2-like and phagocytic phenotype in ILD lungs.** a) Flow cytometry analysis and quantification (percentage and absolute numbers) of CD45<sup>+</sup> lung cells suspension. Monocytes were gated in CD15<sup>-</sup> HLADR<sup>+</sup> cells. Control (n=4), ILD (n=8). b) Flow cytometry staining of CX3CR1, CD206 and MERTK in CD45<sup>+</sup> lung cells suspension. Control (n=4), ILD (n=8). c) Triple immunofluorescence staining of CD14 (white), CD16 (red), and Axl (green). Pictures were taken using magnification of 40x (scale bar= 20µm), white squares represent higher magnification (scale bar= 10µm). Cell nuclei are stained by DAPI (blue).

Control (n=3), ILD (n=3). d) Immunofluorescence staining of CX3CL1 (red) and acetylated tubulin, or collagen type I, or Von Willebrand factor (green), ILD (n=3).

**Figure 7. CX3CR1-fractalkine axis enhances pro-fibrotic non-classical monocyte migration into ILD lungs.** Representative scheme shows an overview of monocyte subsets role and function in healthy (left) and ILD (right) lungs. Non-classical monocytes are decreased in the blood of ILD patients. Diffusing lung capacity of carbon monoxide (DLCO) is decreased in ILD. Fractalkine (CX3CL1) levels are higher in the lungs than in the blood of ILD patients. Fractalkine is expressed by epithelial cells. CX3CR1<sup>+</sup> CD163<sup>+</sup> non-classical monocyte migration is increased in the presence of fractalkine in ILD.

Figure 1

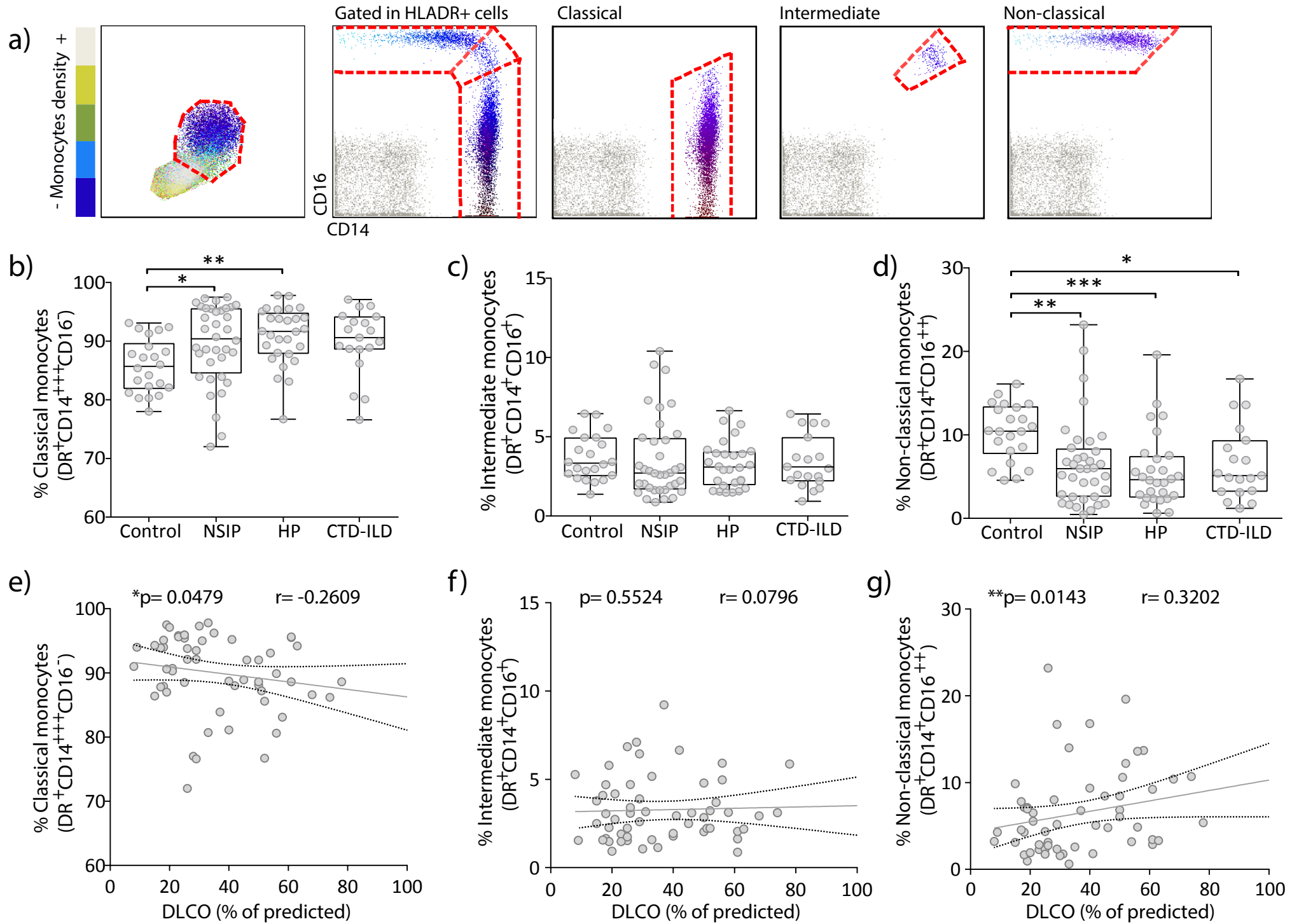


Figure 2

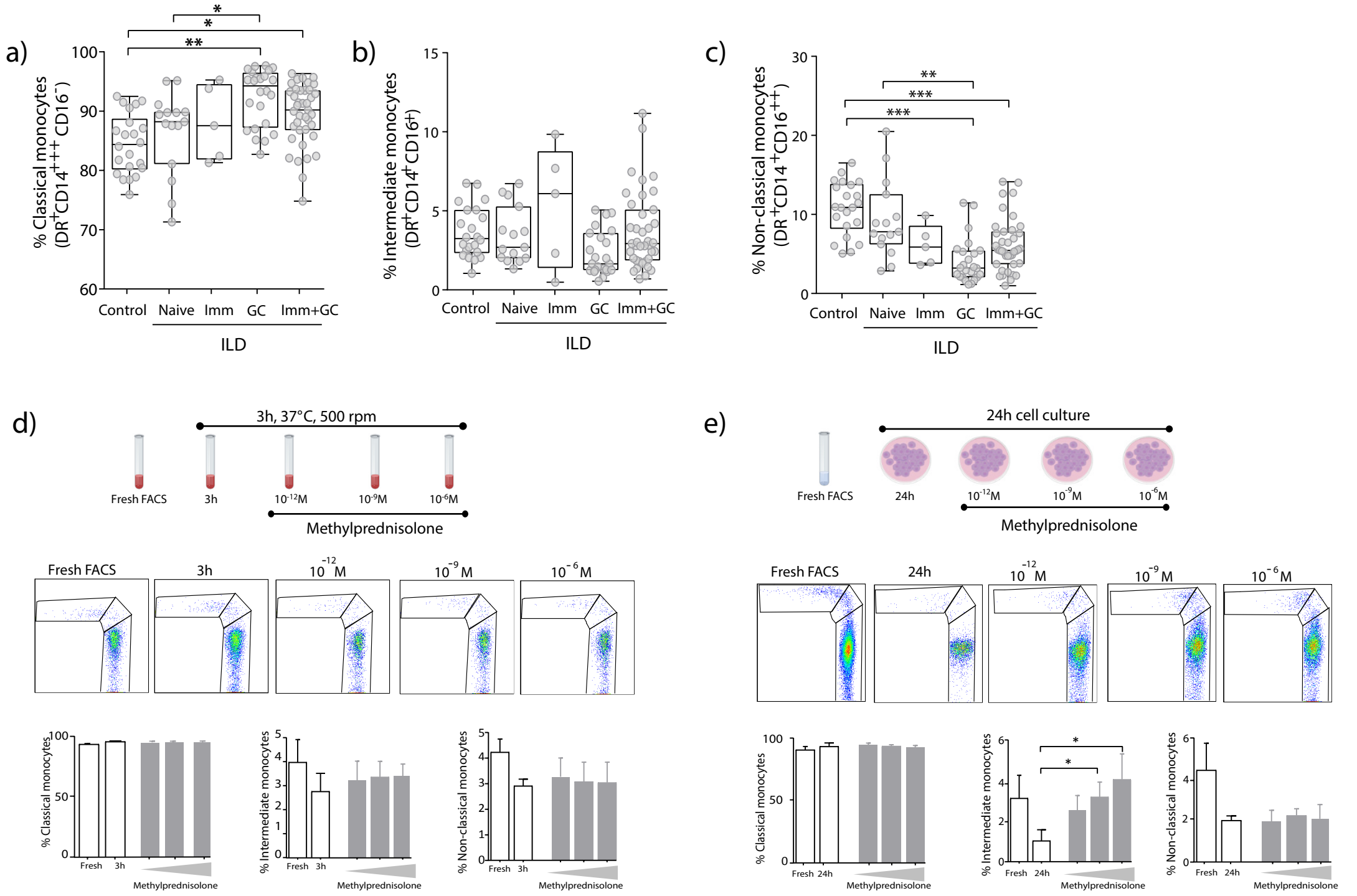


Figure 3

a)   
■ Isotype   
■ Classical monocytes   
■ Intermediate monocytes   
■ Non-classical monocytes

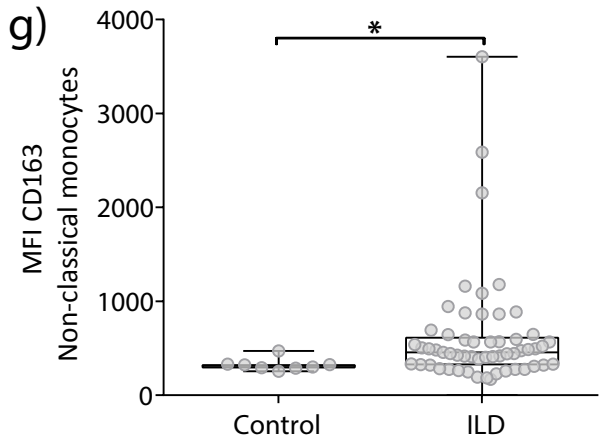
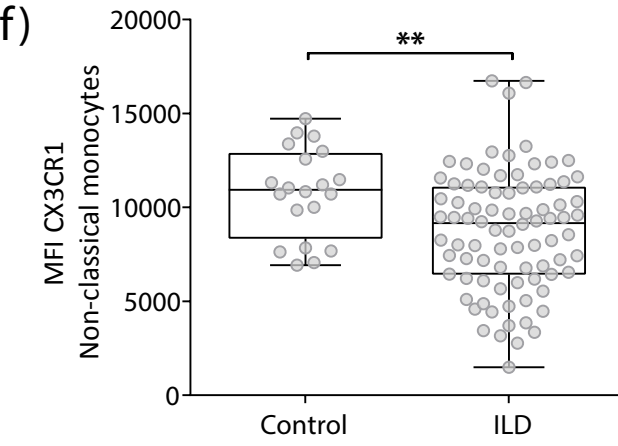
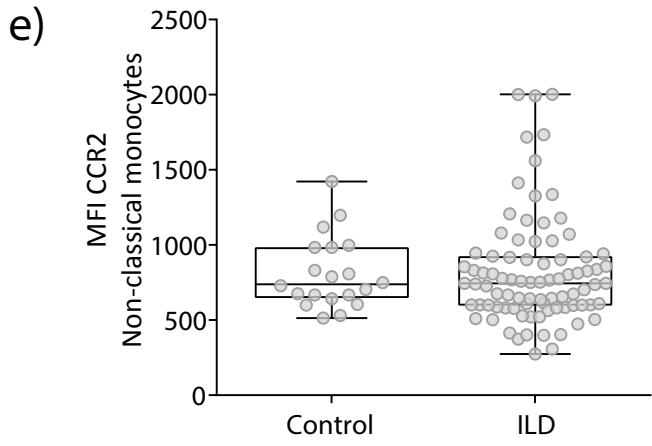
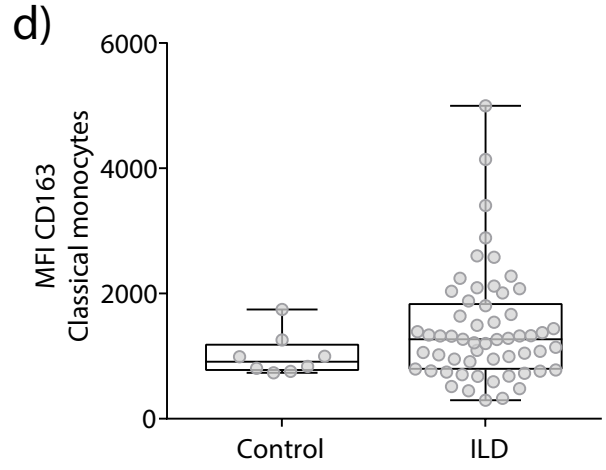
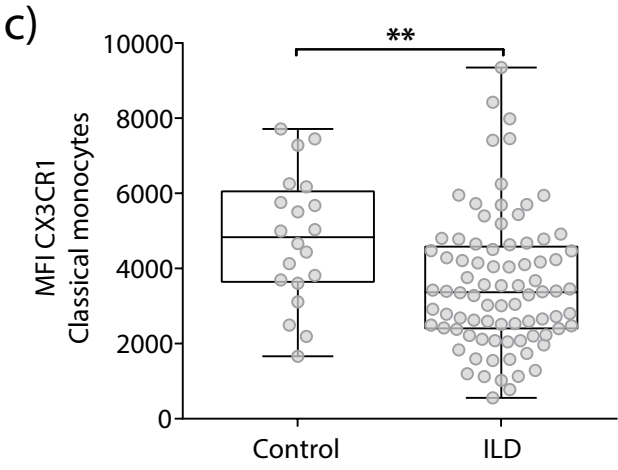
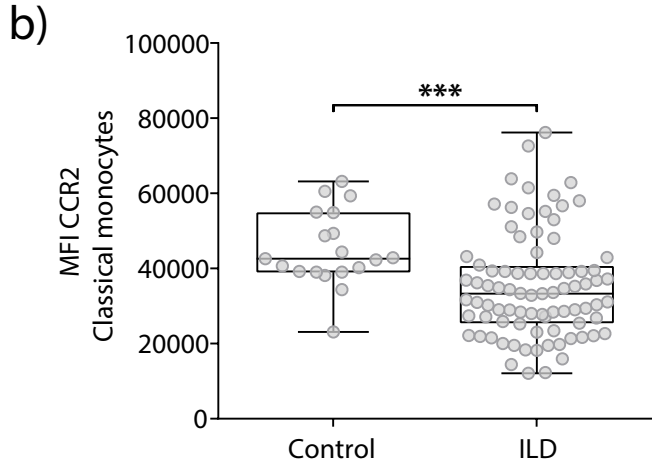
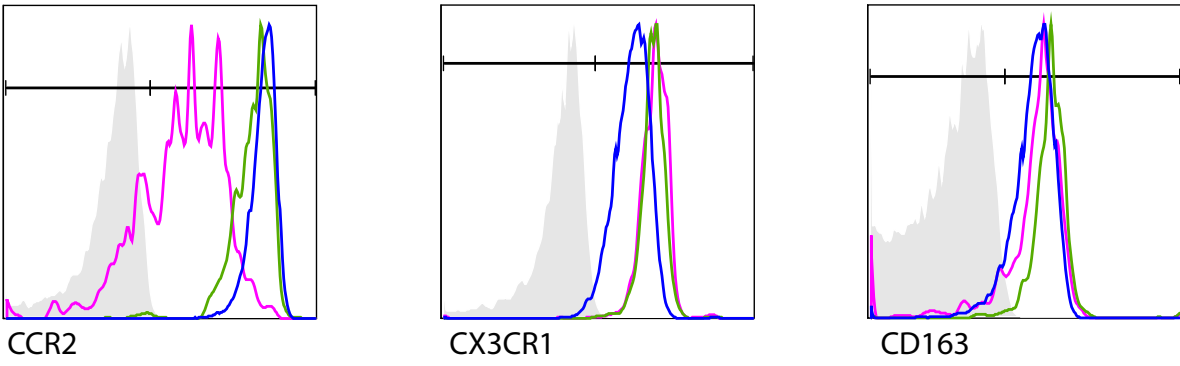
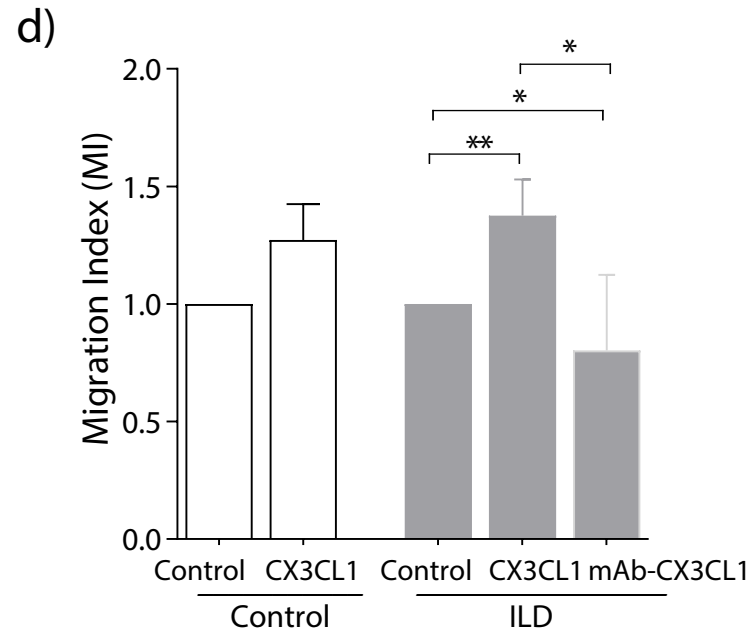
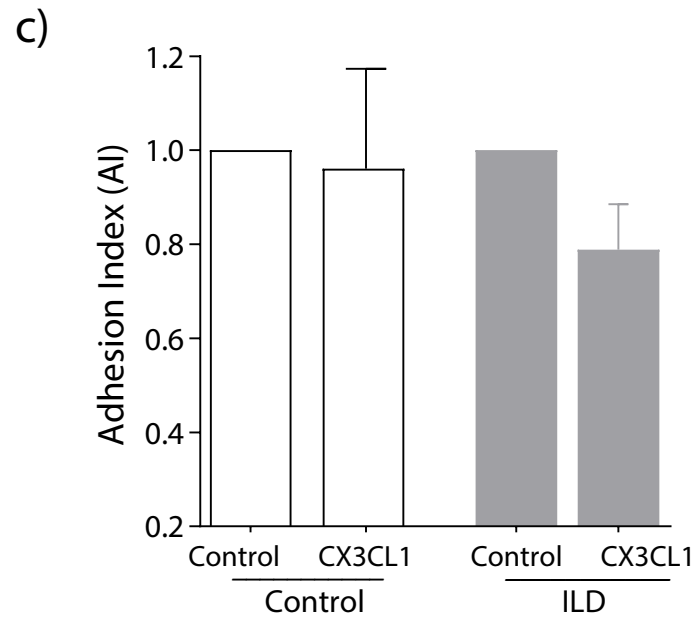
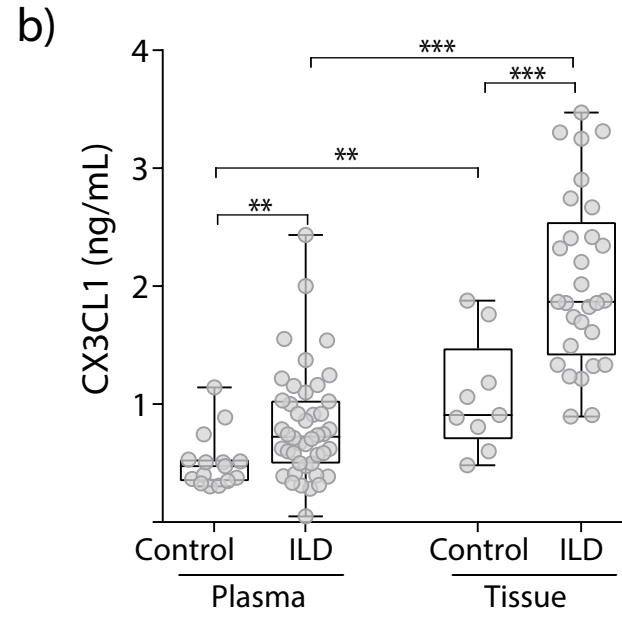
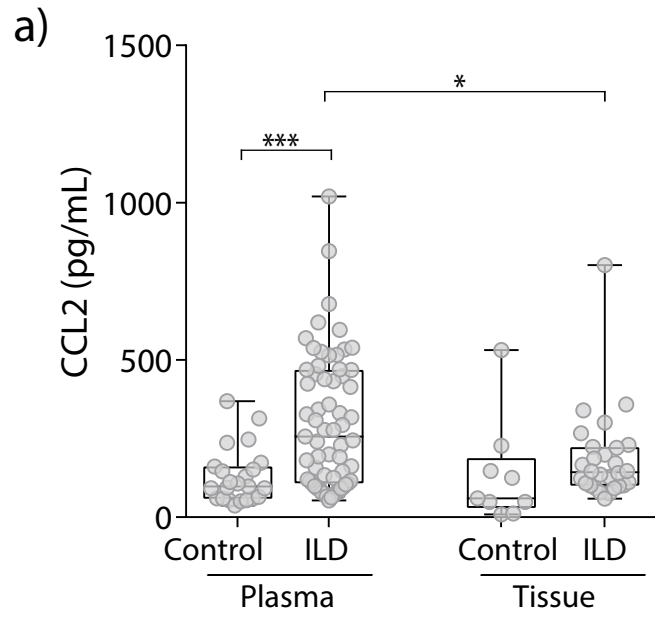


Figure 4



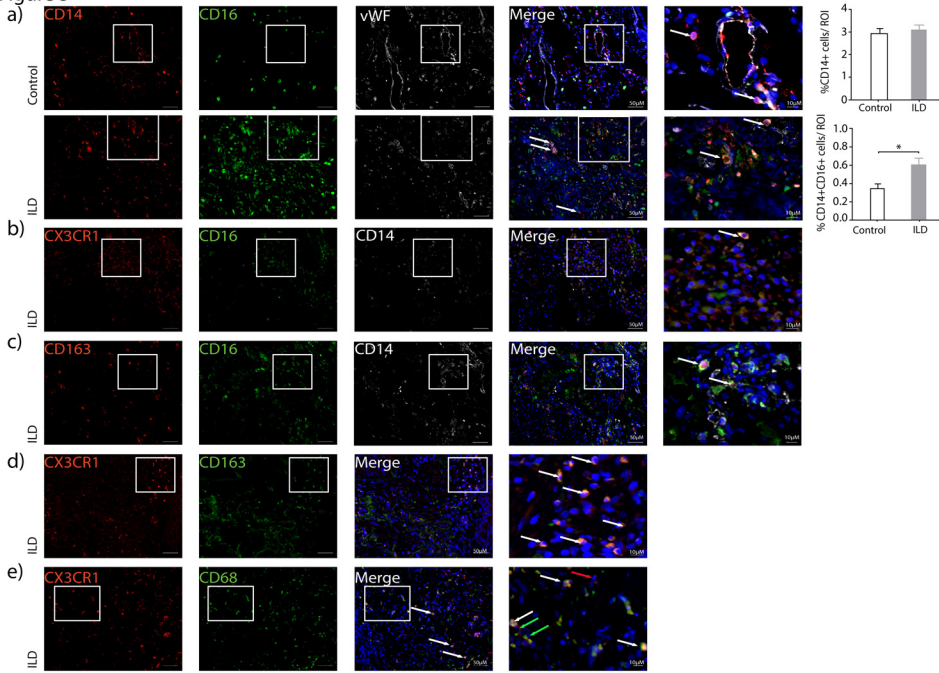
**Figure 5**

Figure 6

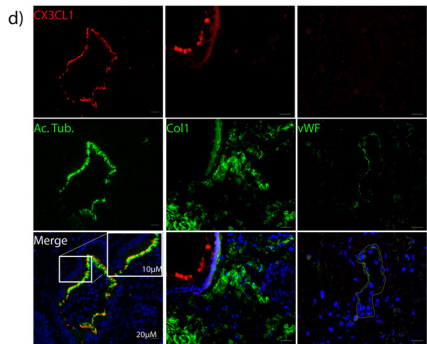
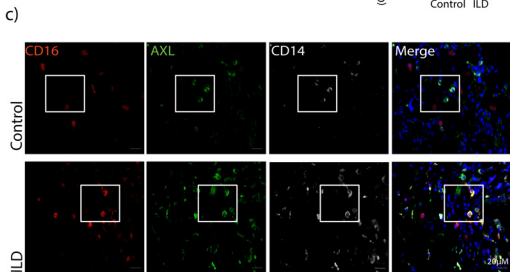
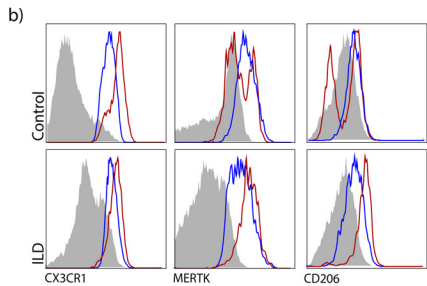
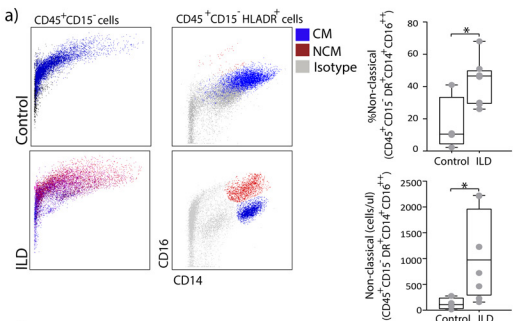
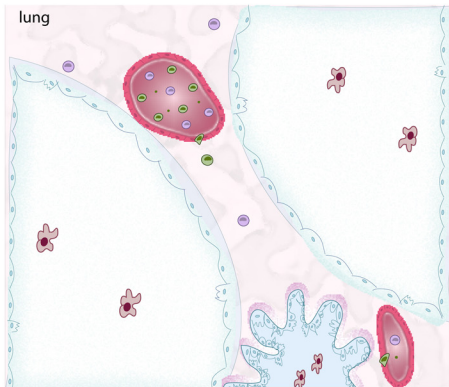


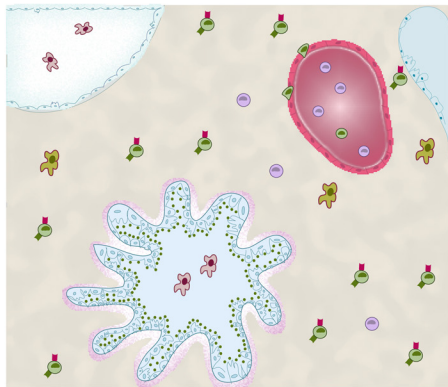
Figure 7

Healthy



ILD

↓DLCO



Fractalkine CX3CL1    Classical monocyte    Non-classical monocyte    CD163    CX3CR1    Alveolar macrophage    Interstitial myeloid cell

**Table 1**

<b>Characteristics</b>	<b>Control</b>	<b>NSIP</b>	<b>HP</b>	<b>CTD-ILD</b>
	22	36	28	19
<b>Age (years)</b>	55.32±7.27	59.78±11.33	61.44±8.33*	65.61±11.09**
<b>Gender</b>				
Female	9 (40.9%)	15 (41.6%)	11 (39.3%)	18 (94.7%)
Male	13 (59.1%)	16 (58.4%)	17 (60.7%)	1 (5.3%)
<b>Smoking Status</b>				
Current	-	1 (2.8%)	-	-
Former	7 (31.8%)	17 (47.2%)	9 (32.2%)	10 (52.6%)
Never	15 (68.2%)	18 (50%)	19 (67.8%)	9(47.4%)
<b>Biopsy</b>	-	63.8% (23/ 13)	32.2% (9/ 19)	5.3% (1/ 18)
<b>Lung comorbidities</b>	-	2.8% (1/ 36)	7.1% (2/ 28)	26.3% (5/ 19)
PAH		-	2	5
CPFE		1	-	-
<b>Treatment</b>	-	83.4% (30/ 6)	89.3% (25/ 3)	68.4% (13/ 6)
Immunosuppressor		3	-	2
Glucocorticoid		12	16	3
Immunosuppressor + glucocorticoid		15	9	8
<b>DLCO (%predicted)</b>	-	34.26±14.22	30.17±17.26	51.06±26.8 <sup>†</sup>
<b>FVC (%predicted)</b>	-	56.91±18.17	55.56±19.52	72.06±18.09 <sup>††</sup>

## ONLINE DATA SUPPLEMENT

### **CX3CR1-fractalkine axis drives kinetic changes of monocytes in fibrotic interstitial lung diseases**

Flavia R. Greiffo, Valeria Viteri-Alvarez, Marion Frankenberger, Daniela Dietel, Almudena Ortega-Gomez, Joyce S. Lee, Anne Hilgendorff, Jürgen Behr, Oliver Soehnlein, Oliver Eickelberg<sup>#\*</sup> and Isis E. Fernandez<sup>#\*</sup>

<sup>#</sup>These authors contributed equally.

<sup>\*</sup>To whom correspondence should be addressed: Isis E. Fernandez, Comprehensive Pneumology Center, Ludwig-Maximilians University and Helmholtz Zentrum München, Max-Lebsche-Platz 31, 81377 München, Germany, Tel.: 0049(89)31871663; Fax: 0049(89)31874661; Email: [isis.fernandez@helmholtz-muenchen.de](mailto:isis.fernandez@helmholtz-muenchen.de), or Oliver Eickelberg, Department of Medicine and University of Colorado, School of Medicine, Aurora, Colorado, Anschutz Medical Campus, 12700 E. 19<sup>th</sup> Avenue, RC 2, Room 9C03, Box C272, 800045 Aurora, CO, USA, Tel.: 001(303)7244075; Fax: 001(303)7246042; Email: [oliver.eickelberg@ucdenver.edu](mailto:oliver.eickelberg@ucdenver.edu)

## **METHODS**

### **Subjects**

The study was performed in accordance with protocols approved by the Ludwig-Maximilians Universität München ethics review board (numbers 180-14 and 454-12). All subjects provided written informed consent for the research study and molecular testing. Hundred-five subjects were included in this study. Of those, were diagnosed with non-specific interstitial pneumonia (NSIP) =36, hypersensitivity pneumonitis (HP) = 28, and connective tissue disease-associated ILD (CTD-ILD) =19), and 22 were control (table 1). The diagnosis of ILD cases were performed by multidisciplinary consensus, based on the current ATS/ERS criteria [1]. Control subjects did not have any signs of active infection, inflammation, and/or respiratory symptoms during blood collection. Tissue samples were obtained from University Hospital Grosshadern and Asklepios Fachkliniken München-Gauting, Munich, Germany. Tissue control samples (tumor-free areas) were obtained from Asklepios Fachkliniken München-Gauting, Munich, Germany.

### **Flow Cytometry**

Fresh venous blood was collected in EDTA-coated vacutainer tubes (Sarstedt; Nümbrecht, Germany), following by the isolation of peripheral blood mononuclear cells (PBMCs) buffy coats prepared by density gradient sedimentation (Lymphoprep™ STEMCELL Technologies; Köln, Germany), where the three subsets of monocytes were detected. PBMCs were stained with monocyte antibody mix containing: anti-human HLA-DR, CD16, CD14, CCR2, CX3CR1 and CD163 (table S1 in the online supplement) for 20 minutes at 4°C in the dark. Monocytes were gated in HLA-DR<sup>+</sup> cells, followed by classification of classical monocytes (CD14<sup>+++</sup>CD16<sup>-</sup>),

intermediate monocytes (CD14<sup>+</sup>CD16<sup>+</sup>), and non-classical monocytes (CD14<sup>+</sup>CD16<sup>++</sup>), and data are presented as % of total monocytes. Canonical markers CCR2, CX3CR1, and CD163 were analyzed in each subset of monocyte and data presented as mean fluorescence intensity (MFI) of total monocytes. For monocytes characterization in the tissue lung, we used lung cells suspension isolated from human lungs. For that, human lungs explants were placed in a 10 cm dish containing DMEM-F12 media supplemented with 20% fetal bovine serum (FBS) and 100 U/mL of penicillin/streptomycin. The lung tissue explants were subdivided into 1-2 mm<sup>2</sup> pieces using scissors or scalpel, and thereafter transferred in a 50 ml falcon tube for further enzymatic digestion with 5 mg of Collagenase I (Biochrom, Germany), for 1 h at 37°C. Then, the digested tissue pieces were filtered through 70um Nylon filters, and washed with 10ml phosphate buffered saline (PBS) for 5 minutes at 450g at 4°C. Cells number was defined by trypan blue staining. Next, lung myeloid cells were isolated using CD45 MicroBeads (Miltenyi Biotec; Bergisch Gladbach, Germany). Subsequently, lung myeloid cells were stained with an antibody mix containing anti-human: CD15, HLA-DR, CD16, CD14, MERTK and CD206. Data acquisition of all flow cytometry analysis was performed in a BD LSRII flow cytometer (Becton Dickinson; Heidelberg, Germany). Data were analyzed using the FlowJo software (TreeStar Inc; Ashland, OR, USA). Negative thresholds for gating were set according to isotype-labeled controls.

### **Methylprednisolone assay**

To investigate the glucocorticoid (GC) effect on monocytes subsets, and understand if GC affect mature monocyte phenotype, we performed experiments with whole blood and isolated monocytes from control and treated them with different doses of GC: methylprednisolone, at 3h and 24hrs, as previously reported [2]. First, 100ul of

whole blood was aliquoted in and methylprednisolone (Sigma-Aldrich; St. Louis, USA) was added in different concentrations:  $10^{-12}$ M,  $10^{-9}$ M and  $10^{-6}$ M. For comparison, an aliquot of 100ul whole blood was not treated with methylprednisolone. Whole blood aliquots were incubated for 3 hours, at 37°C and 500 rpm. After incubation, whole blood was stained with flow cytometry antibody mix containing: anti-human HLA-DR, CD14 and CD16. We used, fresh 100ul of blood for assay control. Isolated monocytes by Pan Monocyte Isolation Kit followed (Miltenyi Biotec; Bergisch Gladbach, Germany) were seeded in 24 wells plate in the following conditions:  $10^{-12}$ M,  $10^{-9}$ M and  $10^{-6}$ M. Next, monocytes were incubated in for 24 hours at 37°C in humidified conditions containing 5% CO<sub>2</sub>. Thereafter, monocytes were harvested and stained with flow cytometry antibody mix containing: anti-human HLA-DR, CD14 and CD16. We used, fresh monocytes for assay control. Data acquisition of flow cytometry analysis was performed in a BD LSRII flow cytometer (Becton Dickinson; Heidelberg, Germany). Data were analyzed using the FlowJo software (TreeStar Inc; Ashland, OR, USA). Negative thresholds for gating were set according to isotype-labeled controls.

### **Protein quantification**

CCL2 and Fractalkine (CX3CL1) (Quantikine Kit R&D Systems, Abingdon, UK) were used to quantify monocytes' chemokines levels in plasma and tissue homogenate. For lung homogenate, human lung tissue were pulverized in liquid nitrogen and homogenized in one volume of lysis buffer (1M Tris HCl pF 7.5, 5M NaCl, 100% NP-40, 10% Sodium-deoxycholat, 0.1% SDS). Samples were subsequently centrifuged at 10,000g for 15 minutes at 4°C, and the supernatant protein express were collect to measure protein levels by BCA Protein Assay Kit (Pierce, ThermoFisher, Rockford,

IL, USA). Protein aliquots containing 100µg total lung were used to measure levels of CCL2, and 200µg total lung were used to measure levels of CX3CL1 [3, 4].

### **Immunofluorescence**

We analyzed explanted lungs from control (tumor-free areas) and ILD patients. Immunofluorescence staining was performed in lung tissue embedded in paraffin. For that, slides were deparaffinized by incubating overnight at 60°C, following by rehydration where slides were twice immersed in xylol (5 minutes, each), transferred to 100% ethanol (2 minutes, each), once in 90% ethanol (1 minute), 80% ethanol (1 minute), 70% ethanol (1 minute), and finally flushed with distilled water (30 seconds) to wash away the ethanol. Next, for antigen retrieval step we immersed the slides in citrate buffer solution (pH 6.0) and placed into a Decloaking Chamber which was heated up at 125°C (30 seconds), 90°C (10 seconds), afterwards the slides slowly cooled down to room temperature. Then, the slides were washed three times in Tris buffer, following by blocking in 5% BSA – Tris buffer solution (1 hour) to prevent non-specific binding. Further, the slides were tripled-stained with anti-human von Willebrand Factor (ab11713, Abcam; Cambridge, UK), CD14 (ab181470, Abcam; Cambridge, UK), CD14 (BAF383, R&D Systems, Abingdon, UK), CD16 (ab109223, Abcam; Cambridge, UK), Fc gamma RIII/CD16 (NBP-42228, Novus Biologicals, Littleton, Colorado, USA), CX3CR1 (ab8021, Abcam; Cambridge, UK), CD163 (NBP2-36494; Novus Biologicals, Littleton, Colorado, USA), CD68 (M0814, DAKO; Glostrup, DK), CX3CL1 (ab89229, Abcam; Cambridge, UK), acetylated tubulin (ab125356, Abcam; Cambridge, UK), collagen type I (600-401-103-0.1, Rockland, Oxfordshire, UK), and AXL (AF154SP, R&D Systems, Abingdon, UK). The primary antibodies were diluted using the antibody diluent (Zytomed Systems, Berlin, Germany), vWF (1:100), CD14 (1:100), and CD16 (1:200), CX3CR1 (1:500), and

CD163 (1:200), CD68 (1:50), CX3CL1 (1:100), acetylated tubulin (1:200), collagen type I (1:200), and AXL (1:200) (table S2 in the online supplement data). The slides were placed in a wet chamber following by adding the primary antibodies (triple staining or double staining), and incubated them at 4°C, overnight. The slides were rinsed three times with Tris buffer, and 1:250 dilution of each secondary antibody (Alexa Fluor 647 donkey anti-sheep, Alexa Fluor 568 donkey anti-mouse, and Alexa Fluor 488 goat anti-rabbit) was applied and incubated at room temperature (1 hour) in the darkness. Slides were counterstained with DAPI (Sigma-Aldrich; St Louis, MO, USA. 1:2500) (1 minute). Once again, the slides were rinsed three times with Tris buffer, and covered with Fluorescence Mounting Medium (Dako, Hamburg, Germany). Images of monocytes were obtained using Axiovert II (Carl Zeiss) and processed using the AxioVision 4.9 software (Carl Zeiss). When cells were quantified, the number of monocytes was indicated as CD14<sup>+</sup>, and CD14<sup>+</sup>CD16<sup>+</sup> cells (CD14 red fluorophore, and CD16 green fluorophore) in the tissue, normalized as % of total cells. Five pictures per slide were taken and double positive cells localized in the parenchyma and outside the vessel, stained for vWF (far red fluorophore), were quantified.

### **Monocyte adhesion assay**

Immortalized murine endothelial cells (SVEC) were cultivated and activated with TNF- $\alpha$  (10ng/mL) for 4 hours, at 37°C in humidified conditions containing 5% CO<sub>2</sub>, as described before [5]. Monocytes were isolated from PBMCs using the Pan Monocyte Isolation Kit followed by CD16 MicroBeads (Miltenyi Biotec; Bergisch Gladbach, Germany), resulting in a separation of CD14<sup>+</sup> and CD16<sup>+</sup> monocytes. We performed a competitive assay where CD16<sup>+</sup> monocytes from ILD patient were labeled with green cell dye (LeukoTracker™, Cell Biolabs, INC.; San Diego, CA, USA), and

CD16<sup>+</sup> monocytes from control were labeled with red cell dye (Red Cell Tracker™ Red CMTPIX dye, Life Technologies; Carlsbad, CA, USA). CD16<sup>+</sup> labeled monocytes were resuspended in three different conditions: chemokine free (PBS 2% FBS), CX3CL1 (PBS 2% FBS + 200ng/mL CX3CL1) and CCL2 (PBS 2% FBS + 200ng/mL CCL2 (Peprotech; Rocky Hill, NJ, USA) (figure S1 in the online data supplement). Subsequently, activated endothelial cells were co-cultured with freshly labeled CD16<sup>+</sup> monocytes from control sample and CD16<sup>+</sup> monocytes from ILD sample (1:1) for 15 minutes at 37°C in humidified conditions containing 5% CO<sub>2</sub>. Non-adherent cells were washed away, and adherent cells were fixed with 4% PFA for 15 minutes at room temperature. Adherent monocytes were imaged using a confocal microscope (LSM710, Carl Zeiss, 10x), and images were acquired by 6x6 tile scan, covering the whole surface area of each well. Adherent CD16<sup>+</sup> monocytes were quantified using Imaris' statistical analysis tool Software (Bitplane; version 8.1.2, Concord, MA, USA), where the total number of spot objects, representing the total number of cells were determined. Data was normalized according to control (chemokine free), and adherent cells were defined by fold change/ adhesion index (AI), as previously reported [6].

### **Monocyte migration assay**

Isolated monocytes were seeded into a transwell (Corning® HTS Transwell® 96 wells permeable 5uM pore; Sigma-Aldrich; Kennebunk, ME, USA). To verify whether the migration of monocyte subsets responded to different stimuli, we had four different conditions in the lower chamber: chemokine free (RPMI 1640 + 0.5% BSA), CX3CL1 (RPMI 1640 + 0.5% BSA + 200ng/mL CX3CL1), monoclonal antibody (mAb)-CX3CL1 (RPMI 1640 + 0.5% BSA + 200ng/mL CX3CL1 + 200ng/mL mAb-CX3CL1) and CCL2 (RPMI 1640 + 0.5% BSA + 200ng/mL CCL2) (figure S1 in the

online supplement). Monocytes were incubated for 3 hours, at 37°C in humidified conditions containing 5% CO<sub>2</sub>. Migratory cells were harvested and stained with an antibody mix containing anti-human: HLA-DR, CD14, and CD16 (table S1 in the online supplement), followed by flow cytometry. Data acquisition was performed in a BD LSRII flow cytometer (Becton Dickinson; Heidelberg, Germany). Data were analyzed using the FlowJo software (TreeStar Inc; Ashland, OR, USA). Negative thresholds for gating were set according to isotype-labeled controls. Data were normalized using control wells (chemokine free) as an indicator of conversion efficiency, fold change/ migration index (MI) [6].

## REFERENCES

1. Travis, W.D., et al., *An official American Thoracic Society/European Respiratory Society statement: Update of the international multidisciplinary classification of the idiopathic interstitial pneumonias*. *Am J Respir Crit Care Med*, 2013. **188**(6): p. 733-48.
2. Frankenberger, M., K. Haussinger, and L. Ziegler-Heitbrock, *Liposomal methylprednisolone differentially regulates the expression of TNF and IL-10 in human alveolar macrophages*. *International Immunopharmacology*, 2005. **5**(2): p. 289-299.
3. Lehmann, M., et al., *Senolytic drugs target alveolar epithelial cell function and attenuate experimental lung fibrosis ex vivo*. *Eur Respir J*, 2017. **50**(2).
4. Kortekaas, K.E., et al., *ACE inhibitors potently reduce vascular inflammation, results of an open proof-of-concept study in the abdominal aortic aneurysm*. *PLoS One*, 2014. **9**(12): p. e111952.
5. Gamrekelashvili, J., et al., *Regulation of monocyte cell fate by blood vessels mediated by Notch signalling*. *Nat Commun*, 2016. **7**: p. 12597.
6. Lo Buono, N., et al., *The CD157-integrin partnership controls transendothelial migration and adhesion of human monocytes*. *J Biol Chem*, 2011. **286**(21): p. 18681-91.

## SUPPLEMENTAL FIGURES LEGENDS

**Figure S1. Monocytes function assays: CCL2 decreased the migration of non-classical monocytes in control.** a) CD16<sup>+</sup> monocytes were isolated and co-cultured with endothelial cells (pre activated with 10ng/ml TNF- $\alpha$ ) for 15 minutes. Non-adherent cells were washed away and adherent cells were fixed with 4% PFA; b) CD16<sup>+</sup> monocytes were quantified using confocal microscopy (LSM710; Carl Zeiss). Adherent cells were normalized from control wells as an indicator of conversion efficiency; c) Adhesion index of assay of CD16<sup>+</sup> monocytes, control wells were used as an indicator of conversion efficiency. Control (n=5) ILD (n=5). d) PBMCs were isolated and added into a transwell (5 $\mu$ M pore membrane); e) After 3 hours cells were harvested for flow cytometry (BD LSRII); Monocytes subsets of migratory cells were normalized from control wells (chemokine free) as an indicator of conversion efficiency; f) . a) Migration index of non-classical monocytes, control wells were used as an indicator of conversion efficiency. Control (n=5), ILD (n=5). For functional assays, 3-5 experimental replicates were use in each experiment. Statistical analysis was performed using non-parametric two-tailed Mann-Whitney t test. \* represents p<0.05 compared with control.

**Figure S2. Monocytes subsets did not correlate with FVC in ILD and expressed decreased CX3CR1 and increased CD163.** The values represent percentage of monocytes subsets correlated with FVC (% predicted); a) classical; b) intermediate; and c) non-classical monocytes. ILD (n= 66). For statistical analysis, p values were calculated by Student's t distribution and Pearson correlation. d) Box and whiskers with dot plot diagrams of flow cytometry analysis show the mean fluorescence intensity (MFI) CCR2<sup>+</sup> intermediate monocytes; d) CX3CR1<sup>+</sup> intermediate

monocytes; e) CD163<sup>+</sup> intermediate monocytes. For D and E: control (n=20), ILD (n=83). For D: control (n= 8), ILD (n= 57). Statistical analysis was performed using non-parametric two-tailed Mann-Whitney t test. \* represents p<0.05 and \*\* represents p<0.01 and compared with control.

**Figure S3. CX3CR1 is not expressed by CD163 cells in control lungs.** a) explanted lungs from control were stained with CX3CR1 (red), and CD163 (green). Positive cells are indicated with squares and arrows. Pictures were taken using magnification of 20x (scale bar= 50µm), and white squares represent higher magnification (scale bar= 10µm); b) isotype control (sheep IgG, rabbit IgG) for control; c) isotype control (sheep IgG, rabbit IgG). Control (n=3), ILD (n=3).

**Table S1. Resources used for flow cytometry, immunofluorescence, ELISA, and cell culture.** List of antibodies and resources used for characterization of human monocyte subsets.

**Table S2. Table of results of figures 1-6.** Values and statistical differences of between groups of figures 1-6.

Figure S1

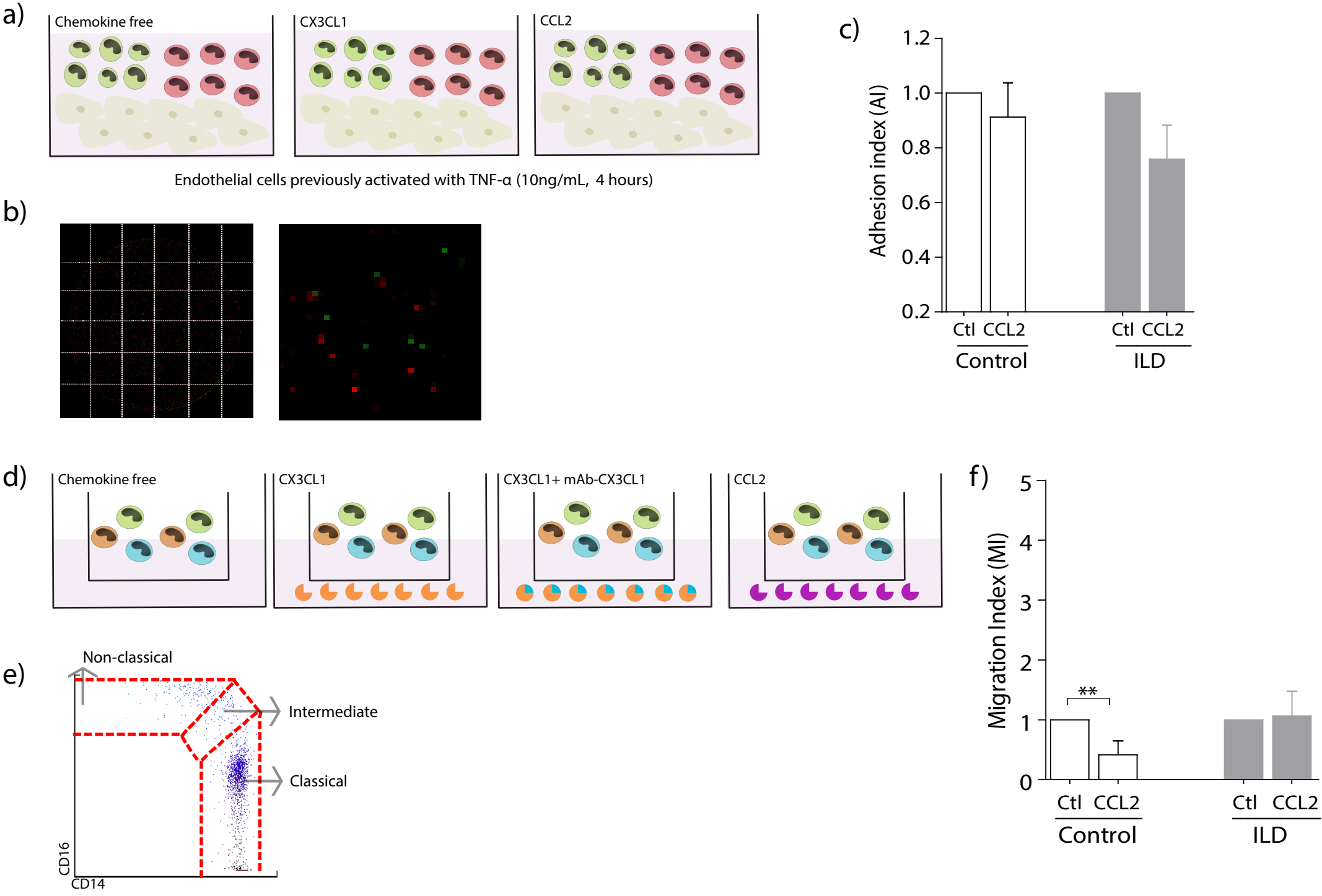


Figure S2

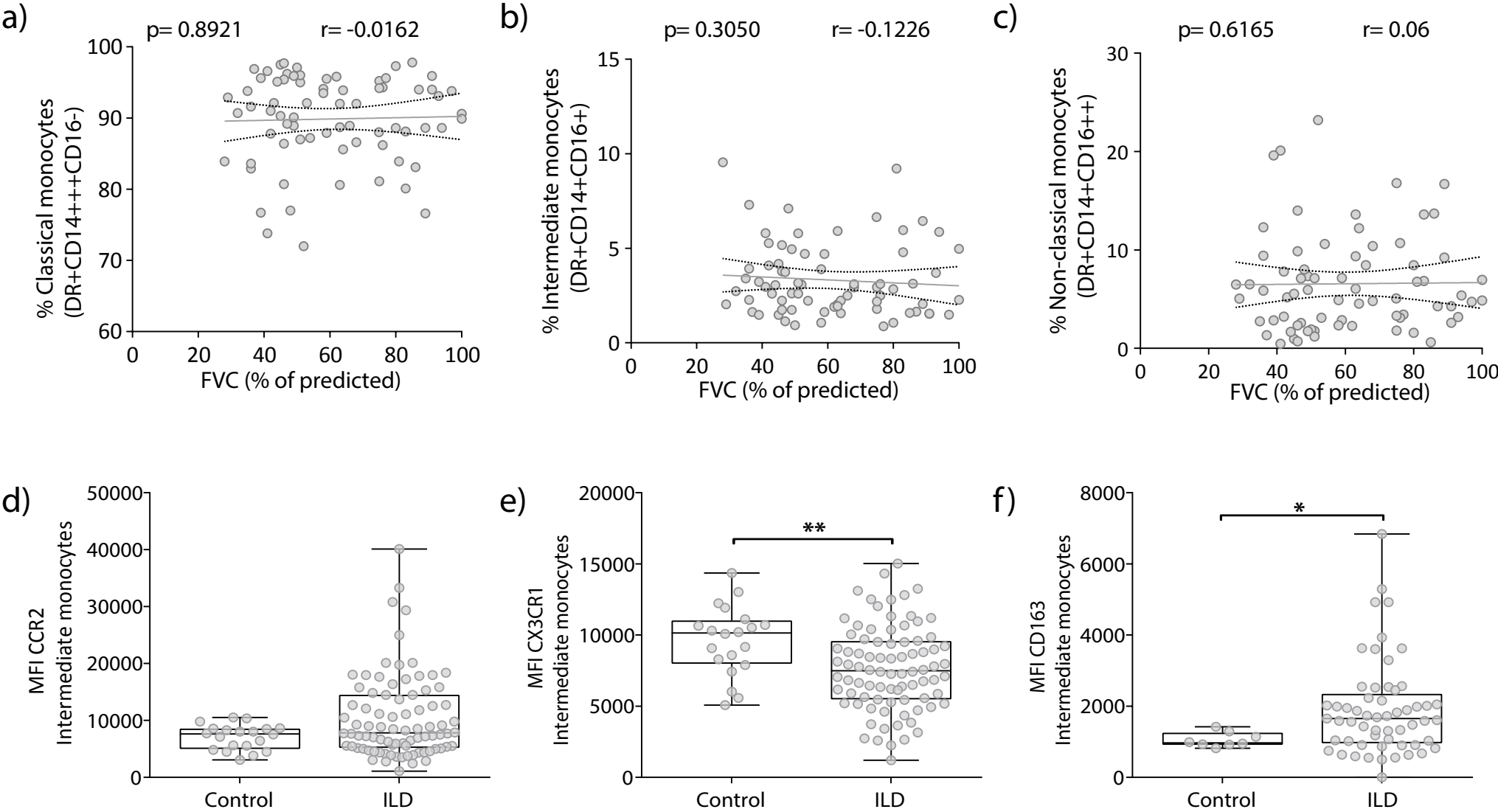
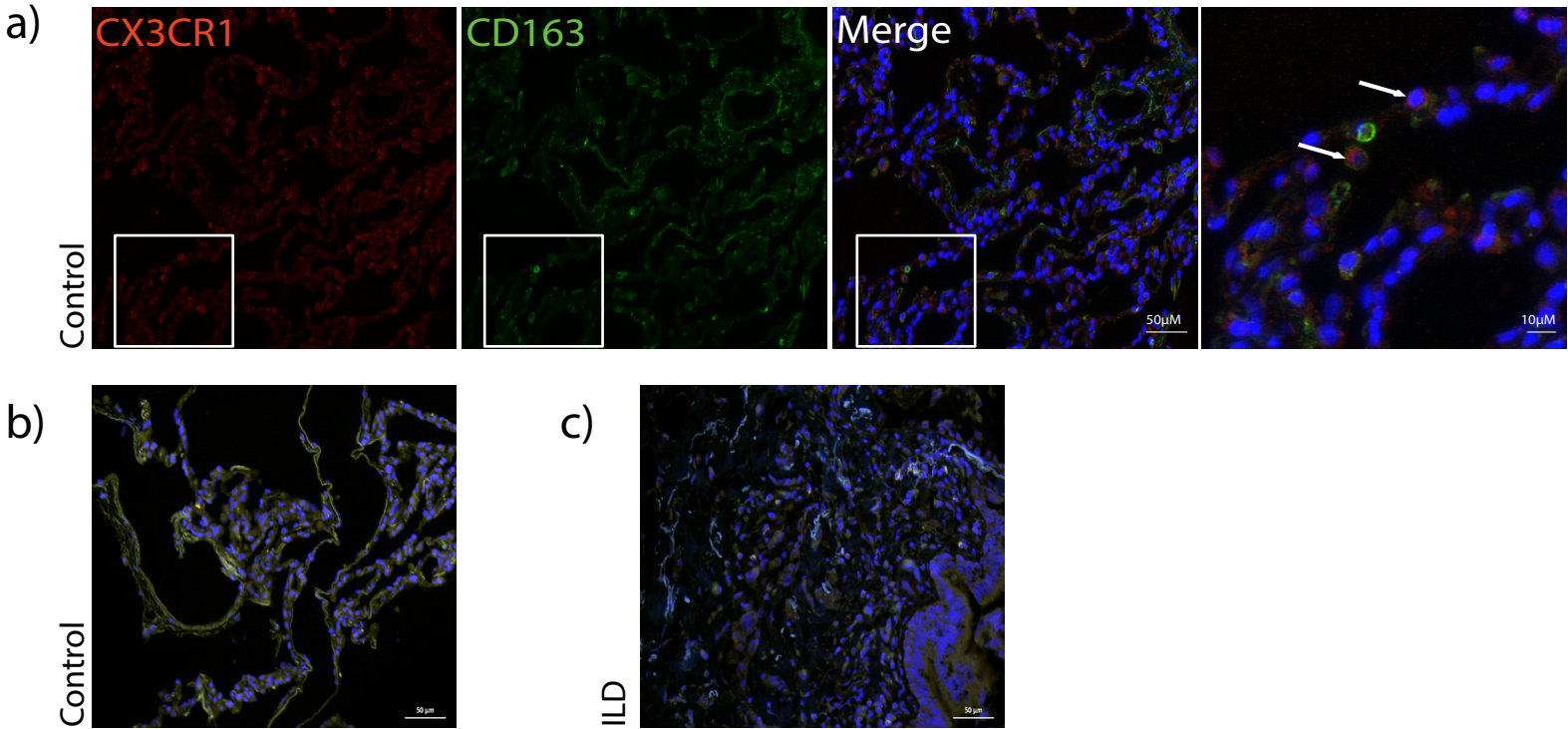


Figure S3



**Table S1**

Reagent	Fluorophore	Isotype	Clone	Manufacturer	Method
HLA-DR	PE-Cy7	Mouse IgG2a	L243	Biolegend	Flow cytometry
CD14	APC-Cy7	Mouse IgG1	HCD14	Biolegend	Flow cytometry
CD16	PerCP/ Cy5.5	Mouse IgG1	3G8	Biolegend	Flow cytometry
CD192 (CCR2)	Brilliant Violet	Mouse IgG2a	K036C2	Biolegend	Flow cytometry
CX3CR1	FITC	Rat IgG2b	2A9-1	Biolegend	Flow cytometry
CD163	PE	Mouse IgG1	GHI/61	BD Biosciences	Flow cytometry
CD15	APC	Mouse IgM	HI98	Biolegend	Flow cytometry
MERTK	Brilliant Violet	Mouse IgG1	590H11G1E3	Biolegend	Flow cytometry
CD206	PE/Cy7	Mouse IgG1	15-2	Biolegend	Flow cytometry
CCL2/ MCP-1	-	-	-	R&D Systems	ELISA
CX3CL1/ Fractalkine	-	-	-	R&D Systems	ELISA
CD14	-	Rabbit IgG	SP192	Abcam	Immunofluorescence
CD16	-	Rabbit IgG	EPR4333	Abcam	Immunofluorescence
Von Willenbrand Factor	-	Sheep IgG	-	Abcam	Immunofluorescence
CD16	-	Mouse IgG2a	5B11	Novus Biologicals	Immunofluorescence
CD14	-	Sheep IgG	-	R&D Systems	Immunofluorescence
CX3CR1	-	Rabbit IgG	-	Abcam	Immunofluorescence
CD163	-	Mouse IgG2b	6E101G6	Novus Biologicals	Immunofluorescence
CD68	-	Mouse IgG1	KP1	DAKO	Immunofluorescence
CX3CL1	-	Mouse IgG1	MM02078J23	Abcam	Immunofluorescence
Tubulin, alpha acetylated	-	Rabbit IgG	-	Abcam	Immunofluorescence
Collagen type I	-	Rabbit IgG	-	Rockland	Immunofluorescence
Axl	-	Goat IgG	-	R&D Systems	Immunofluorescence
Reombinant Fractalkine (CX3CL1)	-	-	-	Peprotech	Cell culture
Anti-Human Fractalkine (CX3CL1)	-	Rabbit IgG	-	Peprotech	Cell culture

All the reagents, and recombinants were qualified for human species.

**Table S2**

<b>Figure 1</b>	<b>Control</b>	<b>NSIP</b>	<b>HP</b>	<b>CTD-ILD</b>
% Classical monocytes (CM)	85.8±4.6	89.5±6.8*	90.9±4.9**	89.8±5.6
% Intermediate monocytes (IM)	3.7±1.4	3.6±2.5	3.2±1.5	3.4±1.7
% Non-classical monocytes (NCM)	10.3±3.4	6.5±5.2**	5.7±4.4***	6.6±4.4*
<b>Figure 2</b>	<b>ILD-Naïve</b>	<b>ILD-Imm</b>	<b>ILD-GC</b>	<b>ILD-Imm+GC</b>
% Classical monocytes (CM)	87.6±6.4	89±5.8	93±4.3**	90.3±4.7*
% Intermediate monocytes (IM)	3.5±1.6	5.1±3.4	2.5±1.3	3.7±2.2
% Non-classical monocytes (NCM)	8.8±4.9	5.6±2.6	3.6±2.9***	3.4±0.5***
<b>Figure 2</b>	<b>Untreated 24h</b>	<b>10<sup>-12</sup> Methylprednisolone</b>	<b>10<sup>-9</sup> Methylprednisolone</b>	<b>10<sup>-6</sup> Methylprednisolone</b>
% Classical monocytes (CM)	93.9±4.6	95.1±2.4	94.1±1.9	93.2±2.4
% Intermediate monocytes (IM)	1.1±1	2.8±1.4	3.5±1.4*	4.4±2.4*
% Non-classical monocytes (NCM)	2±0.4	2±0.9	2.3±0.6	2.1±1.2
<b>Figure 3</b>	<b>Control-CM</b>	<b>ILD-CM</b>	<b>Control-NCM</b>	<b>ILD-NCM</b>
MFI CCR2	45104±10034	35296±13922***	810.6±238	821.4±366.2
MFI CX3CR1	4783±1732	3571±1774**	10785±2394**	8724±3183
MFI CD163	1015±341	1440±894.8	323.5±64.5	612.2±588.4*
<b>Figure 4</b>	<b>Control-plasma</b>	<b>ILD-plasma</b>	<b>Control-tissue</b>	<b>ILD-tissue</b>
CCL2 (pg/mL)	128.7±88.2	301.4±212.5***	134.3±165	185.8±144.4
CX3CL1 (ng/mL)	0.5±0.2	0.8±0.5**	1.1±0.5	2±0.7***